Economic Geology

BULLETIN OF THE SOCIETY OF ECONOMIC GEOLOGISTS

VOL. 113 May No. 3

La Colosa Au Porphyry Deposit, Colombia: Mineralization Styles, Structural Controls, and Age Constraints

Andrés Naranjo,[1,†,*] Johannes Horner,[2] Rudolf Jahoda,[1] Larryn W. Diamond,[3] Adriana Castro,[1] Aura Uribe,[1] Carolina Perez,[1] Hermel Paz,[1] Carlos Mejia,[1] and Jonas Weil[2]

[1] *AngloGold Ashanti Colombia, Carrera 19 Sur 162-70, Ibagué, Tolima 050026, Colombia*

[2] *iC Consulenten, Zollhausweg 1, A5101, Salzburg, Austria*

[3] *Institute of Geological Sciences, University of Bern, Baltzerstrasse 3, 3012 Bern, Switzerland*

Abstract

The La Colosa porphyry Au deposit is located on the eastern flank of the Central Cordillera of Colombia, within the Middle Cauca metallogenic belt. The deposit contains more than 800 t (22.37 Moz) Au at grades up to 0.8 g/t and is hosted by a composite porphyry stock of dioritic to tonalitic composition, which was emplaced into Triassic-Cretaceous schists of the Cajamarca Complex in the late Miocene (~8 Ma).

The country rocks underwent two ductile deformation events, including development of shear zones, folds, and penetrative foliation, prior to emplacement of the stock. Subsequent brittle deformation reactivated preexisting N- and NNE-trending structures and formed secondary faults due to a change from right- to left-lateral shear sense on regional faults. This switch in stress orientations is attributed to a new plate configuration in the mid-Miocene. The left-lateral movement along regional faults favored emplacement of intrusive centers in dilational pull-apart zones, including the La Colosa stock within the regional Palestina fault zone.

The La Colosa porphyry stock was intruded in three stages, termed early, intermineral, and late, all within a relatively short time interval of ~1.1 m.y. The early and intermineral stages are diorite porphyries and related intrusion breccias, whereas the late stage consists of quartz diorite and tonalite porphyries. The intrusions caused contact metamorphism and hydrothermal alteration that partially obliterated the original texture and composition of the schistose country rocks. The early and intermineral stages are dominated by potassic alteration, with local chloritic alteration in the core of the intermineral stage, sodic-calcic alteration in the deeper parts of the stock, and propylitic alteration confined to the late stage.

Three gold mineralization events are recognized at La Colosa. The first was of porphyry style, during which hypersaline fluids (40–50 wt % NaCl equiv) formed predominantly A- and S-type veinlets and caused multistage wall-rock silicification accompanied by potassic and sodic-calcic alteration. The early-stage intrusions contain the highest gold grades varying from 0.75 to 1 g/t Au, associated with pyrite and minor chalcopyrite, molybdenite, and magnetite in the porphyries and with pyrrhotite-pyrite-melnikovite in the country rocks. In the intermineral-stage intrusions the gold grades drop to 0.5 to 0.75 g/t Au, and pyrrhotite and pyrite are the major sulfides. Gold grades reach low values of <0.3 g/t Au in the late-stage porphyries.

The second gold-precipitating event formed sheeted veinlets of drusy quartz and pyrite with centimeter-wide halos of albite-sericite-pyrite overprinting all other alteration types at the deposit. A ~200°C hydrothermal brine (21–28 wt % NaCl equiv) deposited gold at high grades (>1.5 g/t Au over >10 m drill core intervals) within N-striking normal faults that developed during and after emplacement of the porphyry stock. The third mineralization event was supergene, with Au enrichment confined to late porphyries and characterized by sulfide boxworks, resulting in gold grade increases from 0.3 to 1.2 g/t Au.

Introduction

Colombia has been a major gold producer since precolonial times. Currently known gold deposits include orogenic gold, porphyry Cu-Au, porphyry Au, transitional porphyry-epithermal, epithermal, and placer gold (Sillitoe et al., 1982; Rodriguez and Warden, 1993; Sillitoe, 2008). The La Colosa deposit represents a major porphyry gold deposit within the metal-rich Middle Cauca metallogenic belt of Colombia.

The La Colosa deposit, 100% owned and explored by AngloGold Ashanti Ltd, is located 30 km west of the city of Ibague, capital of the Department of Tolima, Colombia (Fig. 1). The

† Corresponding author: e-mail, andres.naranjo@continentalgold.com
*Present address: Calle 7 #39-215, Of. 1208, Medellin, Colombia.

Economic Geology, v. 113, no. 3, pp. 553–578
ISSN 0361-0128; doi: 10.5382/econgeo.2018.4562; 26 p.
Supplementary files available online.

Submitted: April 12, 2017
Accepted: December 22, 2017

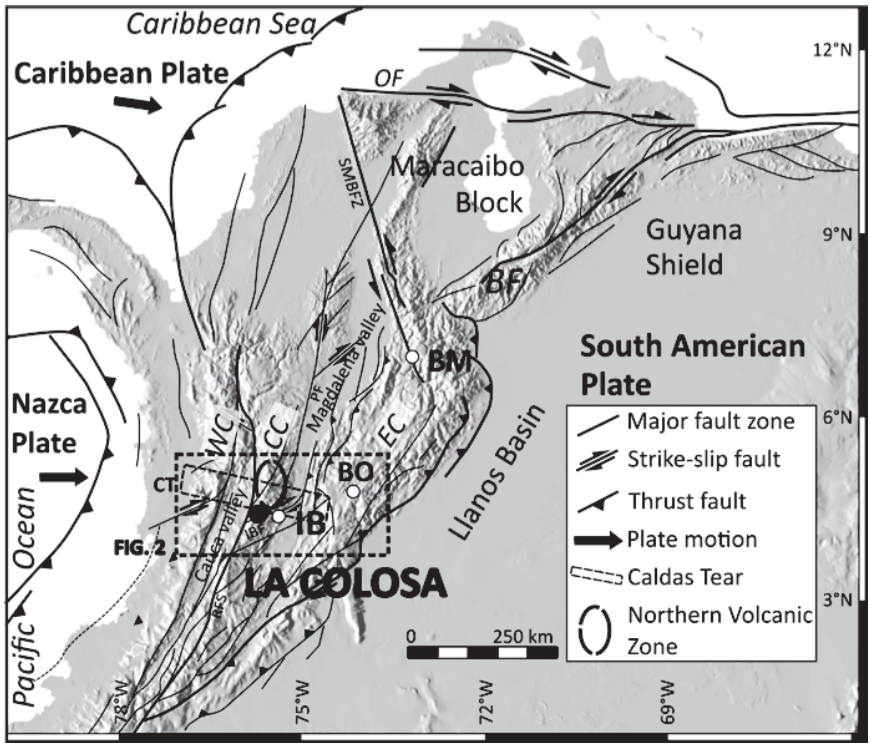

Fig. 1. Digital elevation model (in gray) with location of the La Colosa project and major tectonic features (simplified after Acosta et al., 2004; Cortés and Angelier, 2005; Ingeominas, 2006). Abbreviations: BF = Boconó fault, BO = Bogotá, BM = Bucaramanga, CC = Central Cordillera, CT = Caldas tear (after Vargas and Mann, 2013), EC = Eastern Cordillera, IB = Ibagué, IBF = Ibagué fault, OF = Oca fault, PF = Palestina fault system, RFS = Romeral fault system, SMBFZ = Santa Marta-Bucaramanga fault zone, WC = Western Cordillera.

deposit site is characterized by steep topography on the eastern flank of the Central Cordillera with elevations between 2,300 and 3,500 m above sea level (a.s.l.). The deposit was discovered in 2006 during an extensive greenfields exploration program. Current ore estimates based on 139,000 m of drilling (AngloGold Ashanti, 2016) include an indicated resource of 821 million tonnes (Mt) at 0.85 g/t Au (22.37 Moz) and an inferred resource of 242 Mt at 0.78 g/t Au (6.1 Moz).

Information from surface exposures and drill holes was used to develop the first description of the geology and hydrothermal alteration of the deposit (R. Sillitoe, unpub. report, 2007; Lodder et al., 2010). The present paper integrates new information on rock types, structures, and hydrothermal alteration as well as geochronology and some fluid inclusion analyses. These new data permit constructions of a detailed 3-D model of the deposit, and they provide insights into the structural, magmatic, and hydrothermal events that formed this significant gold deposit in the northern Andes.

Discovery History

In 1984 the Colombian Geological Survey conducted a stream sediment survey in the central part of the Central Cordillera in the Departments of Quindio and Tolima. During this survey, several geochemical anomalies were identified, including an anomalous zone related to the San Antonio gold mine, where minor amounts of gold were exploited from hydrothermal breccias hosted by siliceous schists of the Cajamarca basement complex (Lodder et al., 2010). In 1997, Greystar Resources Ltd. drilled two holes into these hydrothermal breccias, with assays indicating erratic, anomalous concentrations of gold, copper, molybdenum, and arsenic (Lodder et al., 2010).

From 1999 to 2003, AngloGold Ashanti launched a comprehensive greenfields exploration program for porphyry and epithermal gold deposits in the Eastern, Central, and Western Cordillera of Colombia, which included regional database compilation, target generation, and field prospect analysis. The target generation permitted definition of prospective blocks, one of which was the Ibagué-Mariquita block located along the eastern flank of the Central Cordillera, Department of Tolima. Based on the information collected by the Colombian Geological Survey, Greystar Resources, and Conquistador Mines, a visit was made by AngloGold Ashanti to the San Antonio area in 2000 as a part of an agreement with Conquistador Mines. At this time, access to the area was restricted because of unpredictable security conditions. However, during the brief visit, boulders of hydrothermally altered diorite porphyry with porphyry-style veinlets were identified, and the San Antonio area was recommended for follow-up exploration once the security situation allowed it (Lodder et al., 2010).

In 2006, field work started in the Ibagué-Mariquita block with a stream sediment (–200 mesh) sampling program. In this prospective block, several geochemical anomalies were encountered, and the stream sediment sample from La Colosa creek (0.7 g/t Au) was found to be associated with boulders of diorite porphyry containing quartz-sulfide and magnetite veinlets and biotite-rich schist (Lodder et al., 2010). Subsequent

mapping and rock sampling in La Colosa Creek identified two areas with potassic alteration and porphyry-style veinlets. The first diamond drilling program began in February 2007. The initial holes, COL-001 and COL-002, intercepted 138 m with 1.51 g/t Au and 220 m with 1.45 g/t Au, respectively. These findings confirmed that the surface geochemical anomaly persisted at depth and indicated the potential for a >150 t (>5 Moz) gold deposit. Resource drilling continued through to 2016. The continuations of the gold resource to the north and at depth are currently still undefined.

Tectonic Setting of the Northern Andes

In their northernmost extension, the Andes divide into three main branches, the Western, Central and Eastern Cordilleras (Fig. 1). The Western and Central Cordilleras are separated by the Cauca Valley, and the Central and the Eastern Cordilleras are separated by the Magdalena Valley, an intermontane basin. The Llanos basin marks the foreland basin between the Andes and the Guyana Shield.

History of terrane accretion and related magmatism

Each branch of the northern Andes is characterized by its own tectonic history, linked to interactions between the Caribbean, Nazca, and South American plates (Burke et al., 1984; Kellogg and Vega, 1995; Meschede and Frisch, 1998; Cediel et al., 2003). These interactions resulted in complex combinations of subduction, magmatism, terrane accretion, thrusting, and uplift as well as local extension and formation of foreland basins (Aspden and McCourt, 1986; Taboada et al., 2000; Cediel et al., 2003; Corredor, 2003; Moreno-Sanchez and Pardo-Trujillo, 2003; Gómez et al., 2005a, 2005b; Sarmiento-Rojas et al., 2006; Bayona et al., 2008; Nie et al., 2010; Spikings and Simpson, 2014; Mora-Bohórquez et al., 2017). Based on the geologic history, it has been postulated that several terranes accreted episodically to the South American continent between the Cretaceous and the Miocene (Cediel et al., 2003; Restrepo et al., 2011).

The Eastern Cordillera (Chicamocha terrane after Cediel et al., 2003, or Chibcha terrane after Restrepo et al., 2011) is an asymmetric, doubly vergent fold-and-thrust belt of predominantly Mesozoic sedimentary sequences overlying Paleozoic and Precambrian basement rocks (Gómez et al., 2005a, 2005b; Moreno et al., 2011; Van der Lelij et al., 2016). The Central Cordillera contains an eastern terrane (Cajamarca-Valdivia terrane after Cediel et al., 2003, or Tahamí terrane after Restrepo et al., 2011), which is composed of autochthonous Paleozoic basement rocks and volcano-sedimentary sequences of the deformed and metamorphosed Cajamarca Complex (Ordoñez-Carmona et al., 2006; Villagómez et al., 2011; Blanco-Quintero et al., 2014; Martens et al., 2014). Plutonic rocks of Jurassic-Cretaceous age, including the Ibagué and Antioquia batholiths, intruded the basement rocks of the Central Cordillera and reflect magmatic activity during subduction of the Farallon plate (Spikings et al., 2015). The boundary between Chibcha terrane (Eastern Cordillera) and Tahamí terrane (eastern part of the Central Cordillera) is interpreted to be localized along the NE-trending Otu-Pericos and NNE- to N-trending Palestina fault systems (Restrepo et al., 2011; Martens et al., 2014; Mora-Bohórquez et al., 2017).

The authochthonous rocks of the Central Cordillera are divided from the oceanic crust of the Western Cordillera by the Romeral fault zone, a tectonic melange several kilometers wide (Moreno-Sánchez and Pardo-Trujillo, 2003; Villagómez et al., 2011; Mora-Bohórquez et al., 2017). The Romeral fault zone cuts the Cretaceous oceanic arc of the Quebradagrande Complex, which was accreted to the Central Cordillera at about 117 to 107 Ma (Moreno-Sánchez et al., 2008; Villagómez et al., 2011; Blanco-Quintero et al., 2014). The allochthonous Western Cordillera consists of oceanic terranes with predominantly mafic to ultramafic igneous and volcanosedimentary rocks that represent the accreted remnants of the Caribbean large igneous province, which collided with South America at ~75 Ma (Villagómez et al., 2011; Spikings et al., 2015). This collisional event caused the formation of a subduction-related magmatic arc (Bayona et al., 2012), tectonic shortening, the onset of uplift and exhumation of the Central Cordillera, and formation of the foreland basins of the Middle Magdalena basin east of the Central Cordillera during the Paleocene (Nie et al., 2010; Saylor et al., 2010; Borrero et al., 2009; Parra et al., 2012).

The age of major deformation in the Central Cordillera at the latitude of the Middle Magdalena Valley basin is early- to mid-Eocene, as evidenced by the Middle Magdalena Valley unconformity. This regional pediment surface, which developed over approximately 15 m.y., formed during eastward migration of the axis of uplift in the Central Cordillera (Gómez et al., 2005b; Moreno et al., 2011; Parra et al., 2012).

In the Miocene, the Panama-Choco block collided with the Western Cordillera (Barat et al., 2014), producing the present-day northward convexity of Panama. It also induced further uplift of the Central Cordillera, exhumation of deeper crustal levels, and formation of an intermediate-silicic magmatic arc related to eastward subduction of the Nazca plate (Coates et al., 2004; Borrero et al., 2009; Nie et al., 2010; Farris et al., 2011; Barat et al., 2014). The present-day manifestation of ongoing volcanic activity is the Pliocene-Quaternary volcanic belt of the Northern volcanic zone (Fig. 2; Borrero et al., 2009; Londoño, 2016).

Present-day deformation in the Central Cordillera

The Central Colombian block, which is bounded to the south by the Ibagué fault, to the west by the Romeral suture zone, to the east by the Eastern Cordillera, and to the north by the left-lateral Bucaramanga strike-slip fault, is characterized mainly by NE-striking thrust faults and a few SE-trending strike-slip faults (Fig. 1; Corredor, 2003).

Based on analysis of earthquake focal mechanisms and kinematic fault slip data, it has been shown that the ESE-subducting Caribbean plate is still influencing the deformation style to approximately 5° N latitude, inducing left-lateral displacement along major fault systems, such as the Romeral fault system (Ego et al., 1996; Corredor, 2003). According to Vargas and Mann (2013) a W-trending crustal-scale structure, the Caldas tear (Fig. 1), can be inferred by means of earthquake focal analysis. This structure traverses the Cordillera and may be correlated with the northern boundary of the Pliocene-Quaternary Northern volcanic zone.

According to global positioning system (GPS) measurements and geophysical data, eastward subduction of the Nazca plate is continuing with a convergence rate of approximately 6 cm/y relative to stable South America (Fig. 1; Colmenares and

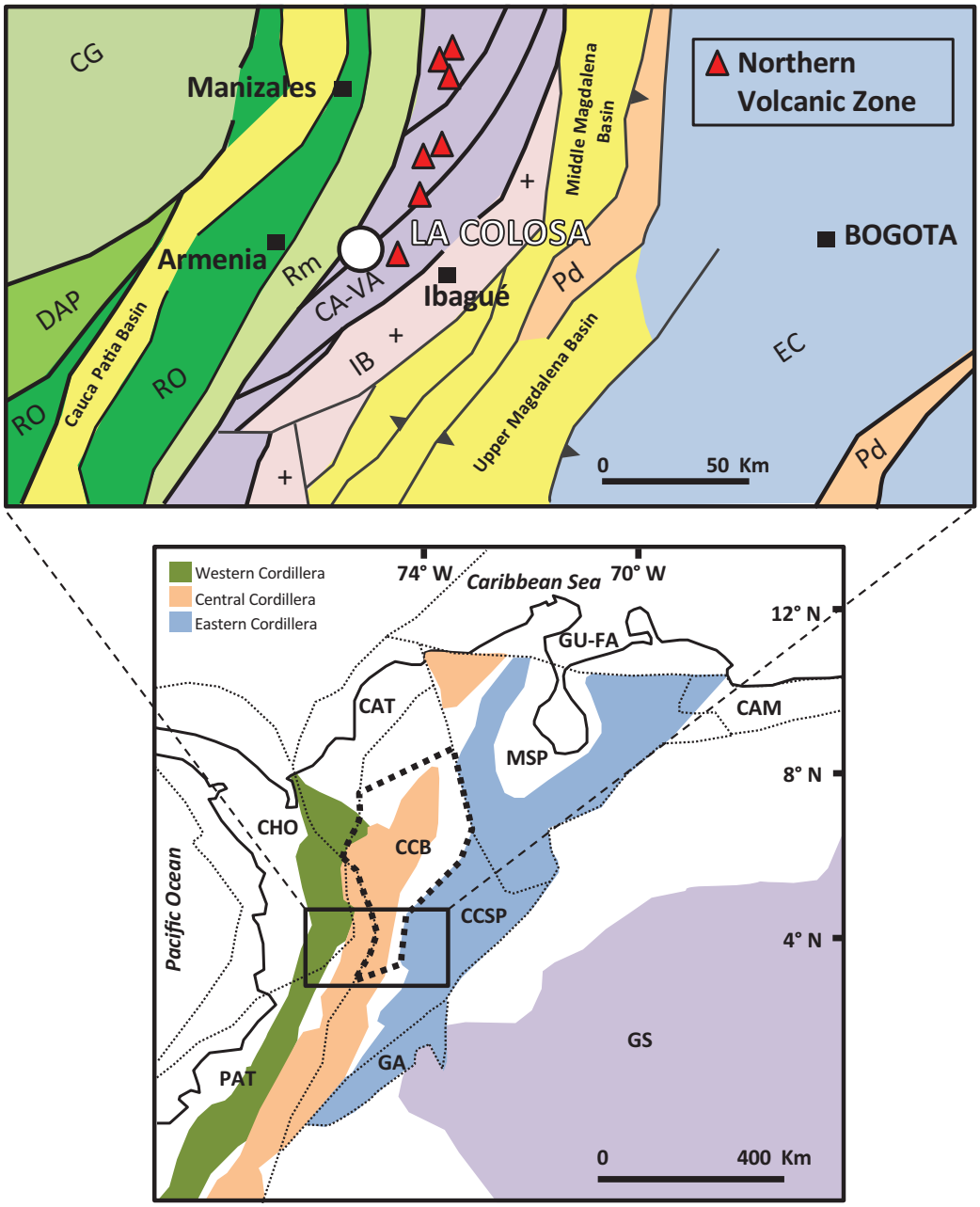

Fig. 2. Tectonic terranes of northwest South America. Abbreviations: CAM = Caribbean Mountain terrane, CAT = Caribbean terranes, CA-VA = Cajamarca-Valdivia, CCB = Central Colombia block, CCSP = Central Continental subplate realm, CG = Cañasgordas, CHO = Choco arc, DAP = Dagua-Piñon, EC = Eastern Cordillera (simplified from Cediel et al., 2003), GA = Garzon massif, GS = Guiana shield, GU-FA = Guajira-Falcon terrane, IB = Ibague block, MSP = Maracaibo subplate, PAT = Pacific assemblages, Pd = Piedemonte, Rm = Romeral mélange, RO = Romeral.

Zoback, 2003; Egbue and Kellogg, 2010). The oblique convergence along the western margin of northern South America causes northeastward sliding of the entire North Andean zone (Ecuador and Colombia) along the major fault systems (Veloza et al., 2012; Alvarado et al., 2016).

Structural Geology and Deformation History at La Colosa

The La Colosa deposit is located east of the continental divide on the crest of the Central Cordillera, between the regionally extensive Romeral fault zone (approx. 6 km to the west of La Colosa) and the Palestina fault system (Fig. 2). Based on differing definitions of tectonic terranes in the Central Cordillera, the La Colosa deposit is located within the Tahamí terrane (Restrepo et al., 2011) or the Cajamarca-Valdivia terrane (Cediel et al., 2003).

La Colosa is situated within a belt of alternating green and black schists and metasedimentary rocks of the Cajamarca Complex. The protoliths of this sequence are interpreted to be a volcano-sedimentary sequence (Blanco-Quintero et al.,

2014). The entire Cajamarca Complex underwent greenschist- to amphibolite-facies metamorphism. In the northern part of the Cajamarca Complex (north and west of the city of Medellín), U-Pb ages indicate that this metamorphism was of Triassic age (U-Pb SHRIMP dating on zircons; Restrepo et al., 2011). However, rocks of the Cajamarca Complex between the city of Ibagué and La Colosa have yielded $^{40}Ar/^{39}Ar$ plateau ages that record a Late Jurassic (157.8 ± 0.6–146.5 ± 1.1 Ma) metamorphic event (Blanco-Quintero et al., 2014).

Based on field observations, drill core data, and published information on the tectonic evolution of the northwestern Andes, the deformation history at La Colosa can be divided into two preporphyry ductile deformation events followed by a syn- to postporphyry brittle deformation event (Horner et. al., 2016; Fig. 3). These are described separately in the following paragraphs.

Ductile deformation

The most obvious feature of ductile deformation D_1 is a penetrative foliation, S_1, which often lies parallel to the original sedimentary layering, S_0. The affected rocks typically display millimeter- to centimeter-wide spacing of individual foliation planes. Crenulation, small-scale folding, and lenses of remobilized quartz are common. The S_1 foliation generally strikes north-south (NW-SE to NE-SW) and dips steeply to the east and west. The predominance of E-dipping foliation planes indicates closed, slightly W vergent folding. Fold axes B_1 plunge subhorizontally to moderately to the north and south. Ductile shear zones are common. They are often oriented parallel or subparallel to foliation S_1; however, their orientation is more variable with strikes to the north, northeast, and northwest. Dips ranges from vertical to shallow.

Locally a second foliation, S_2, can be observed, in particular in the westernmost part of the La Colosa area, approaching the Romeral fault zone and the Quebradagrande Complex. This second ductile deformation event, D_2, overprints S_0 and S_1 (Fig. 3). The second foliation S_2 forms open folds with shallow to moderately dipping limbs; fold axes B_2 show shallow to moderate plunges toward the east and southeast. Shear zones with moderate to shallow dips to the east resemble the axial surface plane of the D_2 fold structures. At or close to ductile shear zones, quartz remobilization, crenulation, and folding are more intense.

Brittle deformation

Brittle deformation (faulting, fracturing, and brecciation) is evident in the metamorphic basement rocks of the Cajamarca Complex as well as in the younger intrusive stocks of the La Colosa area. N-striking faults follow inherited weaknesses at existing ductile shear zones and along fold structures. However, NE- and NW-striking brittle faults are the most prominent brittle structures. The main NE- to NNE-striking structural feature is the regional Palestina fault system, characterized by a series of parallel faults, such as the La Ceja fault or the NE-3 fault (Fig. 4), with minor faults branching off and joining the main fault strands. Based on drilling information, individual faults consist of multiple fault core and damage zones reaching a width of up to 250 m. Kinematic indicators on the NE-striking faults indicate predominantly left lateral and minor right-lateral and normal movement. The N- and NW-striking structures, such as the La Colosa fault, are controlled and limited by the major NE-striking strands of the Palestina fault system. Based on kinematic indicators, these faults display extensional and minor strike-slip characteristics. The geometry of the N- and NW-trending secondary faults and the NE-trending strands of the Palestina fault system and the kinematic relation resemble a sigmoidal-shaped pull-apart structure. At the northern end of the La Colosa area a N-striking structural corridor contains a set of parallel N-striking, E-dipping extensional faults that control high-grade gold mineralization. East- to ESE- and ENE-striking faults and fracture zones are common and represent late-stage extensional deformation, crosscutting the earlier structures.

Characteristics and Sequence of Intrusions and Country Rocks at La Colosa

The La Colosa site contains an intrusive complex with two magmatic centers known as the La Colosa and San Antonio porphyry stocks (Fig. 4), hosted by schistose country rocks of the Cajamarca Complex. The complex is present over a map area of 3.5 km², and it includes a series of porphyry intrusions with compositions ranging from diorite to tonalite. The San Antonio porphyry stock, which lies some 1.5 km to the southeast of the La Colosa stock, includes a late diorite porphyry and hydrothermal breccias (Fig. 4). Whole-rock analyses confirm a medium- to high-K calc-alkaline composition for the La Colosa porphyry stock (Gil, 2010), exhibiting enrichment of large-ion lithophile elements (LILE) and light rare earth elements (LREE) relative to high field strength elements (HSFE) and heavy rare earth elements (HREE), respectively. The $^{143}Nd/^{144}Nd$ (0.512759–0.512870) and $^{87}Sr/^{86}Sr$ (0.707265–0.704510) isotope compositions indicate derivation from a mantle source (Gil, 2010). The concentrations of Nb, Ta, and Ti show negative anomalies, which are characteristic of suprasubduction zone magmatism (Betancourt, 2014).

Three main stages of intrusions make up the La Colosa porphyry complex: early (55–62 wt % SiO_2), intermineral (59–66 wt % SiO_2), and late (61–64 wt % SiO_2) (Gil, 2010). These stages are distinguished by their textures, phenocryst mineralogy, and crosscutting relations, as detailed in the following.

La Colosa early porphyry

The early intrusions occupy a surface area of ~0.35 km² and include five diorite porphyries (E0, E1, E2, EDM, and E3) and three early intrusion breccias (EBX1, EBX2, and EBXDM) (Fig. 4). Early porphyry E0 (Fig. 5A), which is observed only in drill core, is characterized by 20 to 30 vol % of plagioclase and hornblende phenocrysts in a microcrystalline groundmass. Diorite porphyry E1 is equigranular (Fig. 5B), fine to medium grained, with a crowded texture and 60 to 70 vol % of plagioclase, amphibole, and orthoclase phenocrysts. Diorite porphyry E2 is medium to coarse grained with 20 to 30 vol % of subhedral to euhedral plagioclase and hornblende phenocrysts (Fig. 5C). The EDM porphyry is a fine- to medium-grained diorite with 40 to 50 vol % of subhedral to euhedral plagioclase, hornblende, and biotite (Fig. 5D). The last early diorite porphyry, E3, is fine grained, with 30 to 40 vol % of anhedral to subhedral plagioclase phenocrysts (Fig. 5E). E3 intruded the earlier porphyries and generated intrusion breccias (*sensu* Sillitoe, 1985), such as EBX1

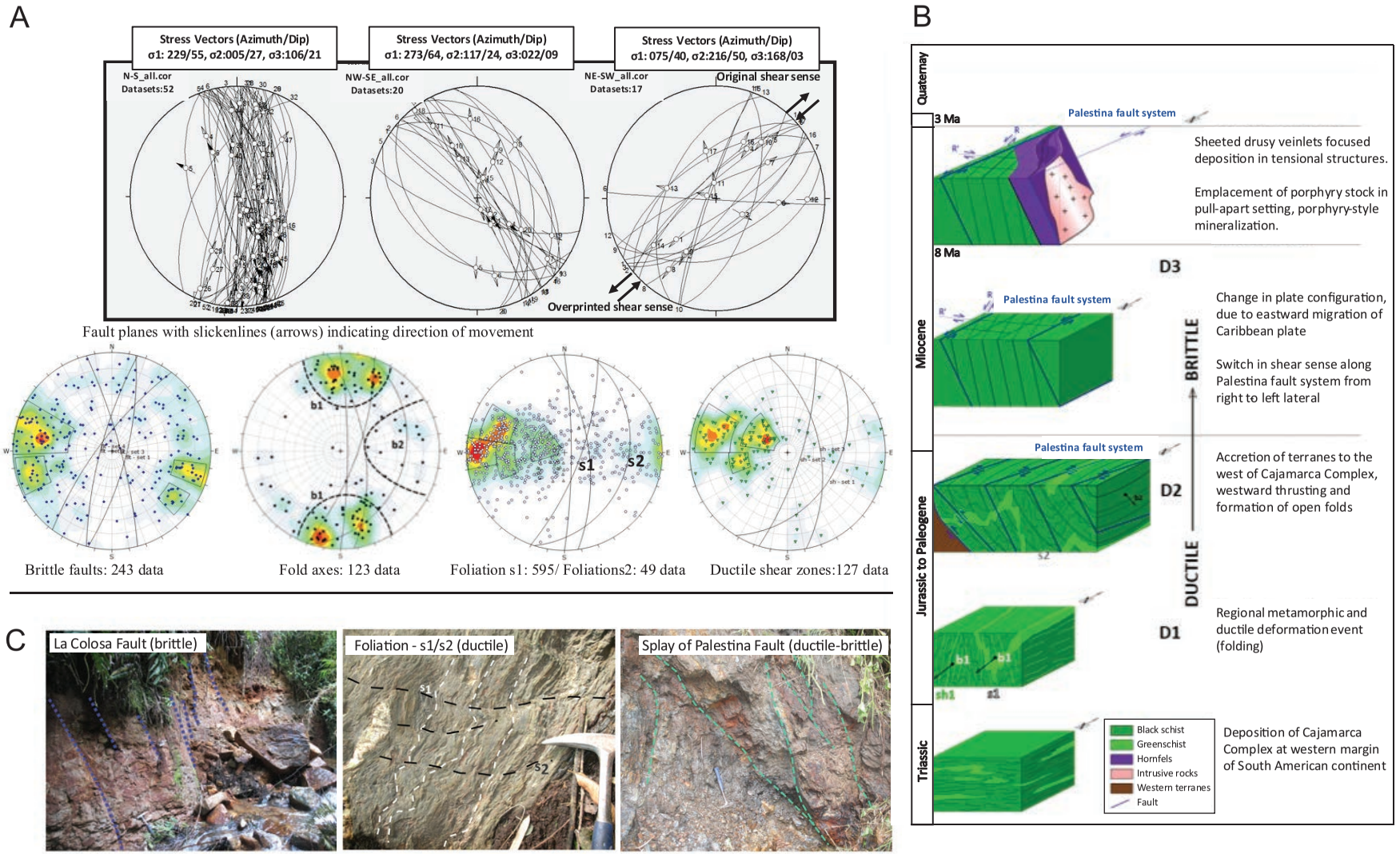

Fig. 3. A. Structural data of the La Colosa project area and paleostress analysis of slickenside data (stereographic projection, lower hemisphere). B. Block diagram illustrating the structural evolution of the area (modified after Horner et al., 2016). C. Outcrops of La Colosa showing ductile and brittle formation.

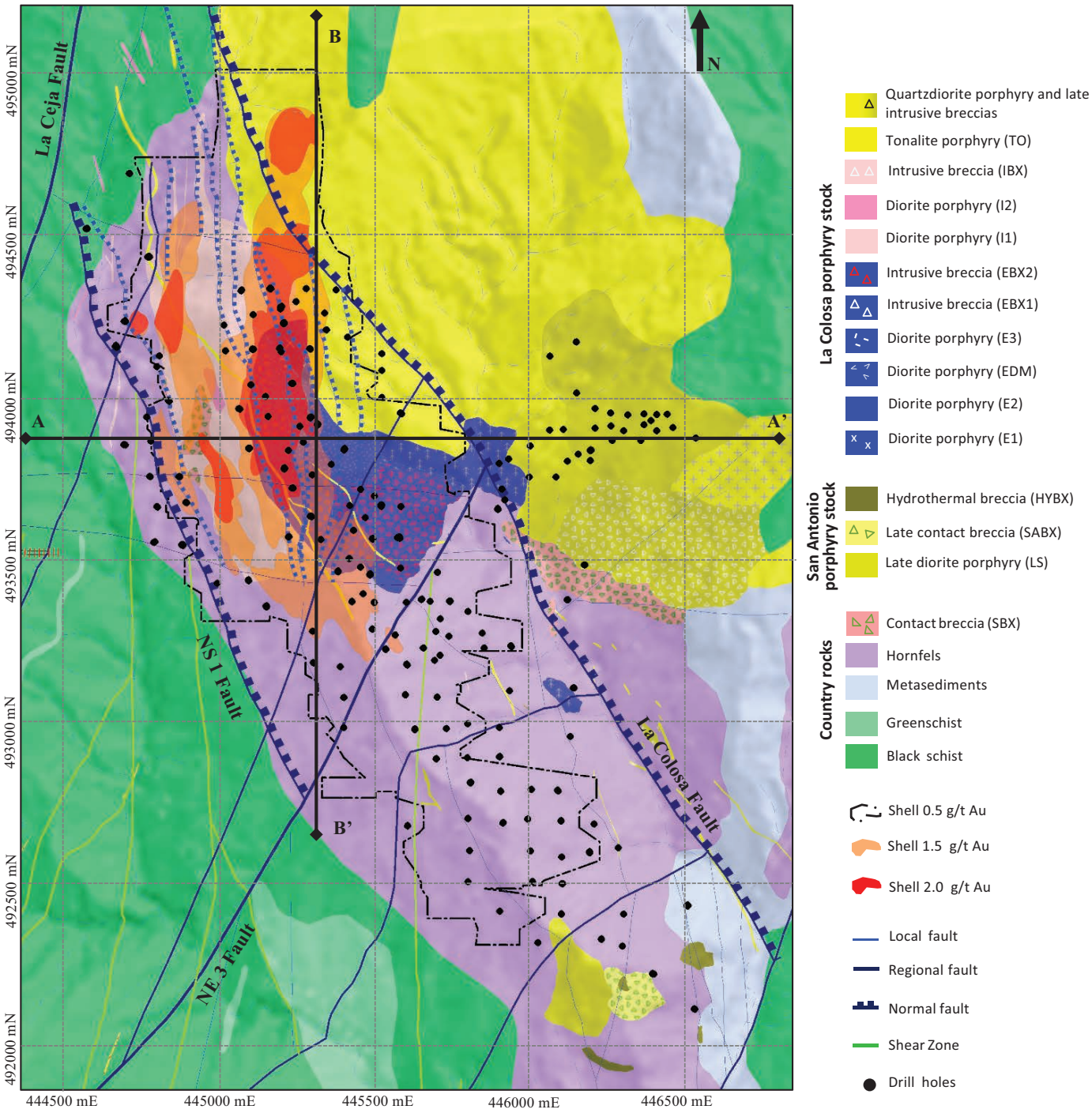

Fig. 4. Geologic map of La Colosa Au-porphyry deposit, illustrating intrusion stages and pulses of La Colosa porphyry stock, country rock, faults, and gold-grade envelopes. Based on drilled boreholes and surficial exposures mapped by La Colosa geology department and IC-Consulenten, 1:5,000 scale. A-A' = east-west profile (439000 mN), B-B' = north-south profile (445300 mE) (WGS 84 UTM zone, 18N projection).

(with E1-dominant clasts; Fig. 5F), EBX2 (with E2-dominant clasts; Fig. 5G), and EBXDM (with EDM-dominant clasts) cemented by porphyritic E3 diorite (Fig. 5H).

La Colosa intermineral porphyry

Two intermineral stocks have been distinguished, covering a total map area of over 0.33 km² (Fig. 4). The earlier of these, I1, is a porphyry with subhedral plagioclase and hornblende phenocrysts (Fig. 5I). The later stock, I2, is a diorite porphyry containing 20 to 30 vol % of subhedral to euhedral plagioclase and hornblende phenocrysts (Fig. 5J). Crosscutting relationships show that I2 intruded I1 and thereby formed intrusion breccia IBX (Fig. 5K). The coarse-grained early-stage and intermineral diorite porphyries are difficult to distinguish

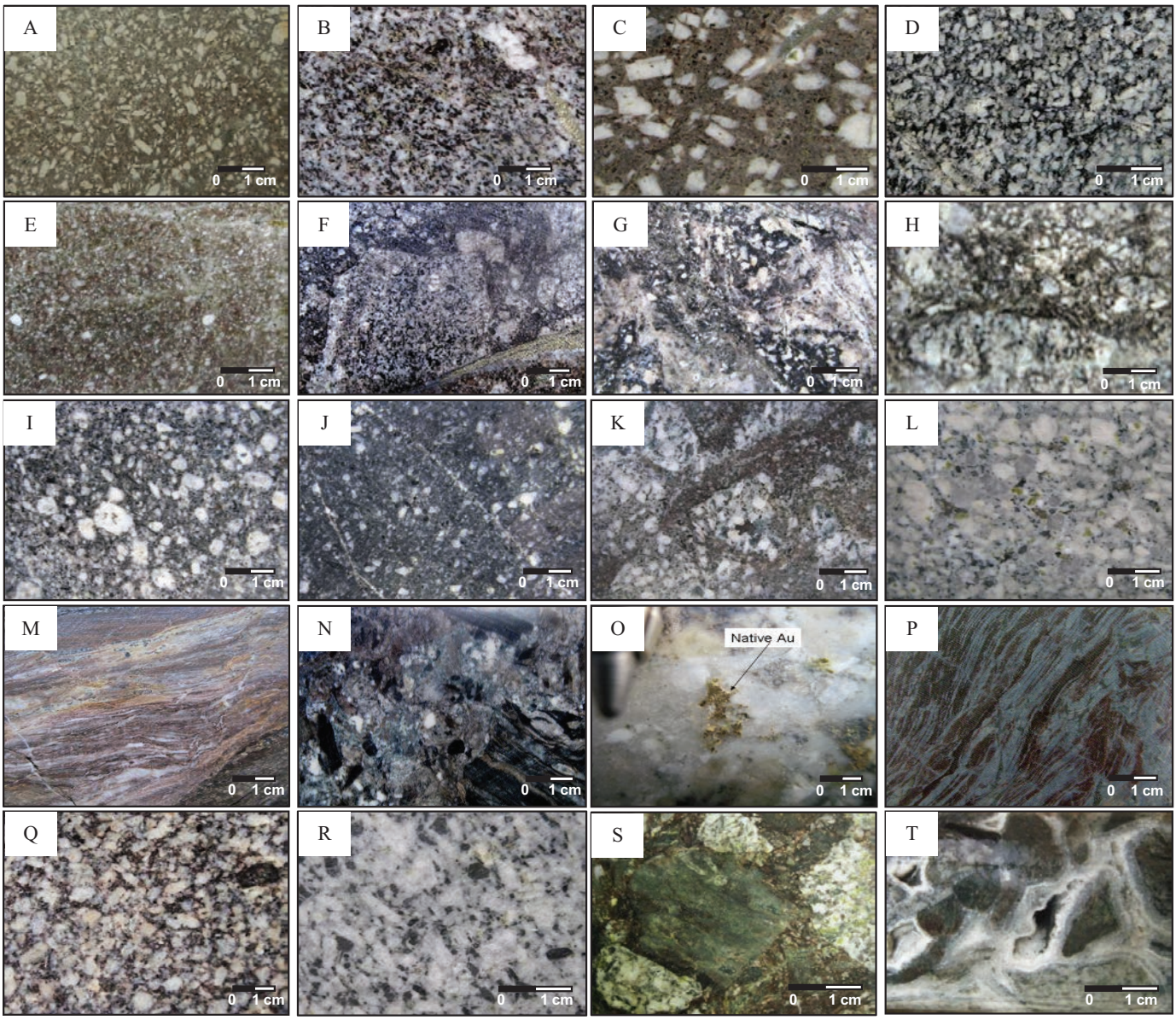

Fig. 5. Photographs of rock units at La Colosa deposit. A. Fine- to medium-grained diorite porphyry (E0). B. Crowded texture diorite porphyry (E1). C. Coarse-grained diorite porphyry (E2). D. Medium-grained diorite porphyry (EDM). E. Fine-grained diorite porphyry (E3). F. Intrusive breccia (EBX1). G. Intrusive breccia (EBX2). H. Intrusive breccia (EBX2). I. Medium- to coarse-grained diorite porphyry (I1). J. Fine- to medium-grained diorite porphyry (I2). K. Intrusive breccia (IBX). L. Coarse-grained tonalite porphyry. M. Schistose wall rock with bands of secondary biotite and albite patches. N. Contact breccia (SBX). O. Free Au COL010 at 328.9 m in coarse-grained diorite porphyry (I1). P. Schistose wall rock with secondary biotite and actinolite-chlorite bands. Q. Coarse-grained diorite porphyry at San Antonio. R. Coarse-grained diorite with propylitic alteration at San Antonio. S. Subrounded to subangular clast of contact breccia (SABX) at San Antonio. T. Hydrothermal breccias with clast of schistose wall rock cemented by quartz + carbonates at San Antonio.

due to their compositional and textural similarities. The main distinguishing criteria, following Sillitoe (2000), are the lower alteration intensity, lower veinlet density, and lower gold contents of the intermineral diorites.

La Colosa late porphyry

The late porphyry stage at La Colosa has a map extent of ~2.7 km², and it is made up of diorite (LD), quartz diorite (QZD), and tonalite (TO) porphyries as well as intrusion breccias (QZDBX), some along the contact with country rock schist (DBX; Fig. 4). The principal rock is the tonalite porphyry (TO) with phenocrysts of plagioclase, quartz, biotite, and hornblende (Fig. 5K), located in the northeast corner of the La Colosa Complex (Fig. 4). This rock also occurs as NW-striking, subvertical to E-dipping dikes cutting the early porphyry intrusions and schistose country rocks and following existing faults, which formed within the pull-apart structure (Fig. 4).

San Antonio porphyry stock

The San Antonio porphyry stock (Fig. 4) is divided into three late diorite porphyry intrusions (LS, IS1, and IS2). Their mutual contacts and their contacts with the schistose country rocks are marked by intrusion breccias (SABX) characterized by subangular clasts of wall rock, IS1, and IS2, cemented by late diorite porphyry LS (Fig. 5S). The last phase of the San Antonio stock consists of hydrothermal breccias (HYBX) containing subangular to subrounded clasts of wall rock and minor diorite in a rock-flour matrix that is locally cemented by sulfides or carbonate minerals (Fig. 5T).

Country rocks

The country rocks at La Colosa are regionally metamorphosed black schists, green schists, and metapelites of greenschist-facies grade. The emplacement of the La Colosa and San Antonio porphyry stocks caused contact metamorphism that transformed the proximal country rocks into hornfels (Lodder et al., 2010), thereby obliterating the original volcano-sedimentary layering of the protoliths.

3-D model of lithologic units

Figure 6 shows the 3-D configuration of all the lithologic units described above, based on surface mapping and core logging. For simplicity, rock types have been grouped as follows: early (early porphyries and early intrusion breccias EBX1, EBX2, and EBXDM), intermineral (intermineral porphyries and intrusion breccia IBX), late (tonalite and quartz diorite porphyries), and wall rock (surrounding schistose country rock and intrusion breccias along its contacts with porphyries SBX).

Distribution of Hydrothermal Alteration and Sulfides in the La Colosa Deposit

Based on surface mapping, detailed core logging, and previous work (Lodder et al., 2010), eight broad mineral assemblages of hydrothermal alteration are distinguished macroscopically (Fig. 7): Sodic-calcic (albite + actinolite ± epidote; Fig 7A);

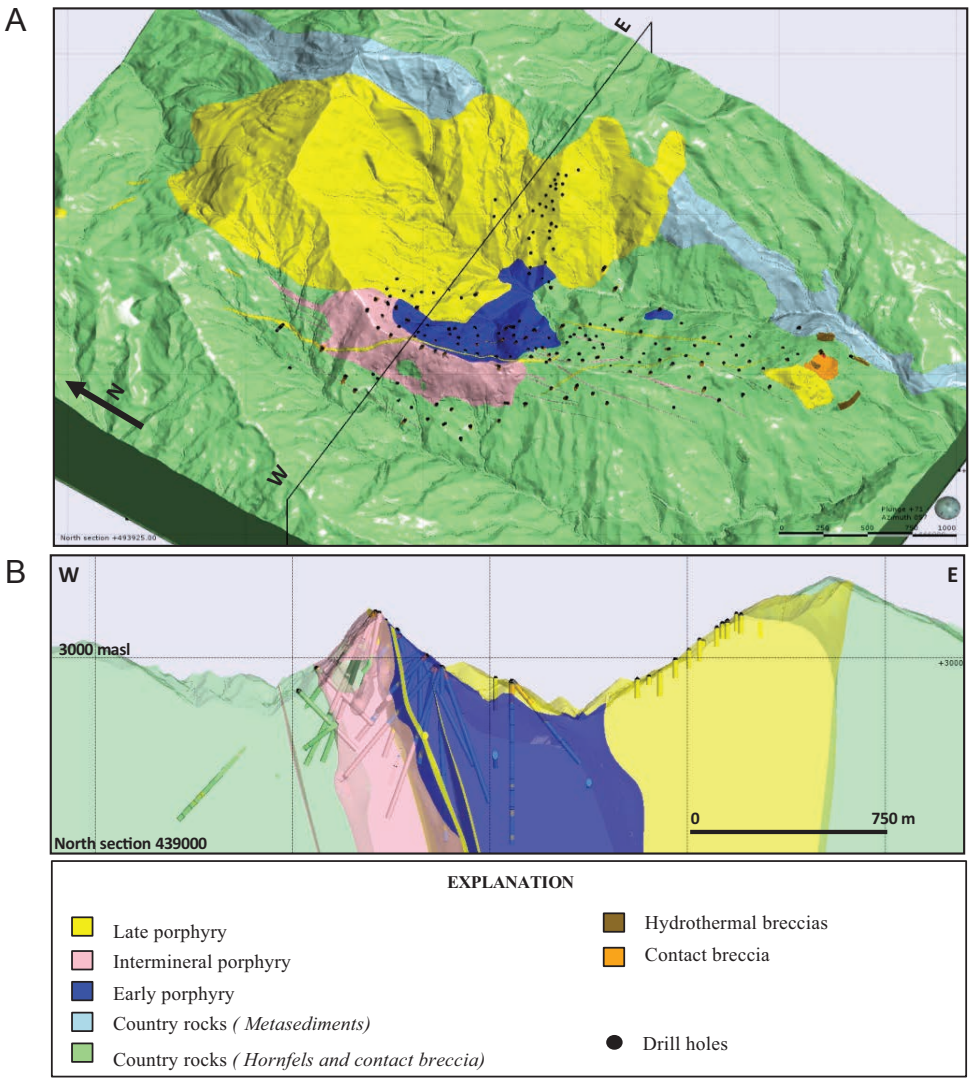

Fig. 6. A. La Colosa 3-D lithology model and B. W-E cross section (looking north) along line 493900 N showing the geologic distribution of early, intermineral, and late intrusive stages of La Colosa Au-porphyry and drilled boreholes. Section thickness 200 m (WGS 84 UTM zone, 18N projection).

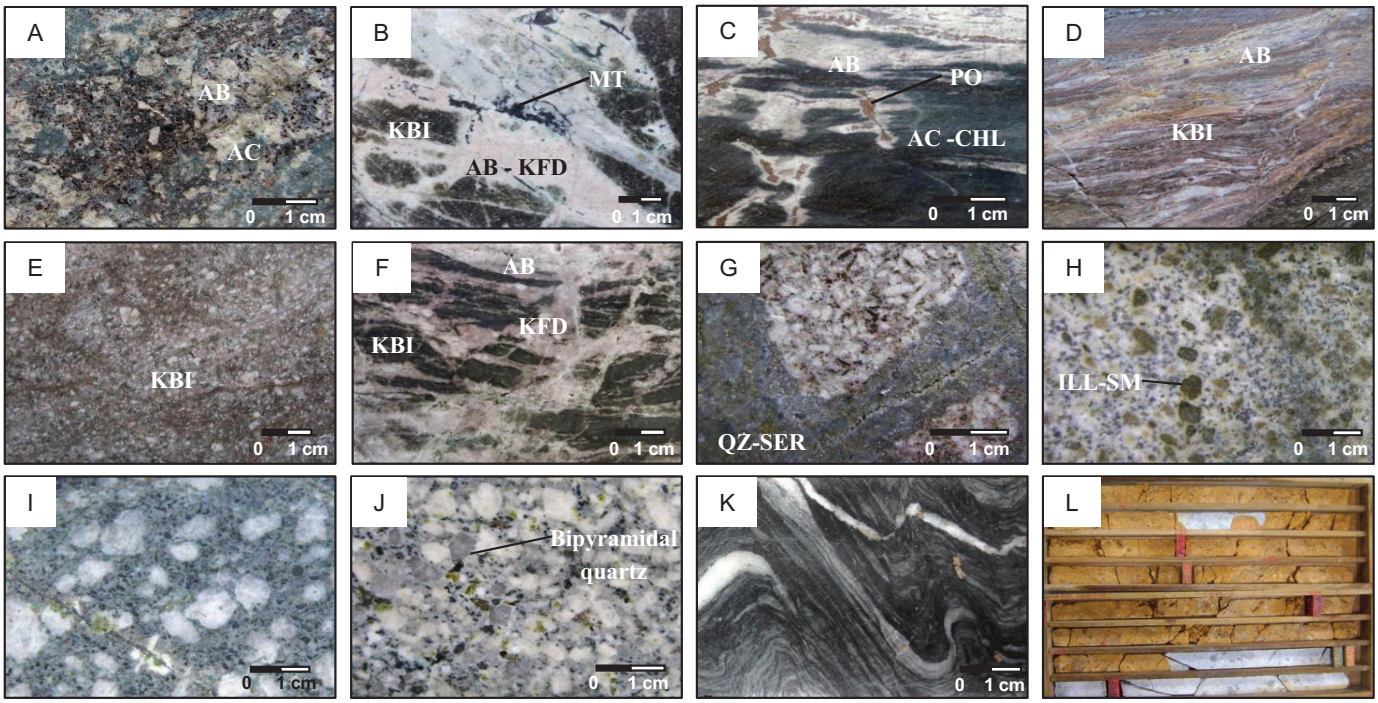

Fig. 7. Photographs of hydrothermal alteration of La Colosa deposit. All samples are from boreholes. A. Sodic-calcic alteration (albite-actinolite assemblage) overprinted by secondary biotite. B. Secondary biotite with patches of albite ± K-feldspar accompanied by magnetite. C. Schistose country rock altered to actinolite-chlorite with patches of albite accompanied by pyrrhotite. D. Schistose country rock altered to secondary biotite with albite patches. E. Fine-grained diorite porphyry with dominant secondary biotite. F. Schistose country rock with patches of albite ± K-feldspar. G. Secondary biotite overprinted by quartz-sericitic alteration. H. Illite-smectite (intermediate argillic alteration) over plagioclase phenocryst. I. Chloritic alteration. J. Propylitic alteration (chlorite-epidote) of tonalite porphyry with bipyramidal quartz phenocryst. K. Schistose country rock with silicification. L. Core box showing clay and Fe oxides. Abbreviations: AB = albite, AC = actinolite, CHL = chlorite, KBI = secondary biotite, KFD = secondary K-feldspar, ILL-SM = illite-smectite, MT = magnetite, PO = pyrrhotite, QZ-SER = quartz-sericite.

potassic (biotite ± K-feldspar), which occurs mainly as vein infill and as pervasive replacement of wall-rock ferromagnesian minerals, such as biotite and hornblende (Fig. 7B, E, F); quartz-sericitic (white to gray mica + quartz; Fig. 7G), which results in partial destruction of the original rock textures; chloritic (chlorite alone; Fig. 7I), which is a late-stage alteration replacing biotite and amphibole; propylitic (chlorite + epidote ± albite ± calcite ± actinolite; Fig. 7J); intermediate argillic (smectite + illite), which overprints the early alteration types, forming patches and selvages (Fig. 7H); silicification (Fig. 7K); and supergene argillic Fe oxide alteration (kaolinite + iron oxides and oxyhydroxides), which is a weathering product showing boxwork textures after sulfide minerals (Fig. 7L).

The 3-D distribution of these alteration assemblages is shown in Figure 8. The various stages of porphyries and the country rocks show distinctive alteration patterns and sulfide mineral assemblages. At the La Colosa intrusive center the predominant type of hydrothermal alteration in the early porphyries is moderately intense potassic alteration (secondary biotite ± K-feldspar). This alteration type with pyrite as the predominant sulfide is locally restricted to the upper part of the early intrusive stage. The deepest members of the early stage, the EDM porphyry and EBXDM breccia, are dominated by sodic-calcic alteration (as centimeter-scale patches and halos around quartz and magnetite veinlets) with subordinate potassic alteration. The early-stage sulfides are pyrite, chalcopyrite, and molybdenite accompanied by hydrothermal magnetite.

The intermineral stocks and breccias are dominantly altered by potassic (secondary biotite) and sodic-calcic assemblages (again confined to centimeter-scale patches and halos around quartz and magnetite veinlets) with some cores of chloritic alteration. Pyrite is the most abundant sulfide, followed by pyrrhotite, which is commonly found close to the contacts with the country rocks. The dominant hydrothermal alteration types in the late porphyries are propylitic followed by intermediate argillic.

Hydrothermal alteration of the San Antonio intrusions is predominantly propylitic with relicts of secondary biotite and sodic-calcic alteration. In contrast, the hydrothermal breccias are dominated by intermediate argillic alteration. Disseminated sulfides include pyrrhotite and pyrite with sporadic occurrences of arsenopyrite, chalcopyrite, and molybdenite. Melnikovite (colloidal pyrite) has been identified as a breakdown mineral after pyrrhotite.

The metamorphic country rocks are partially overprinted by hydrothermal potassic alteration (Fig. 5M) that extends along foliation planes. Less abundant alteration types are several stages of silicification and localized sodic-calcic alteration (Fig. 5P).

In contrast to the other alteration types, quartz-sericitic alteration is clearly structurally controlled: it is spatially limited to a

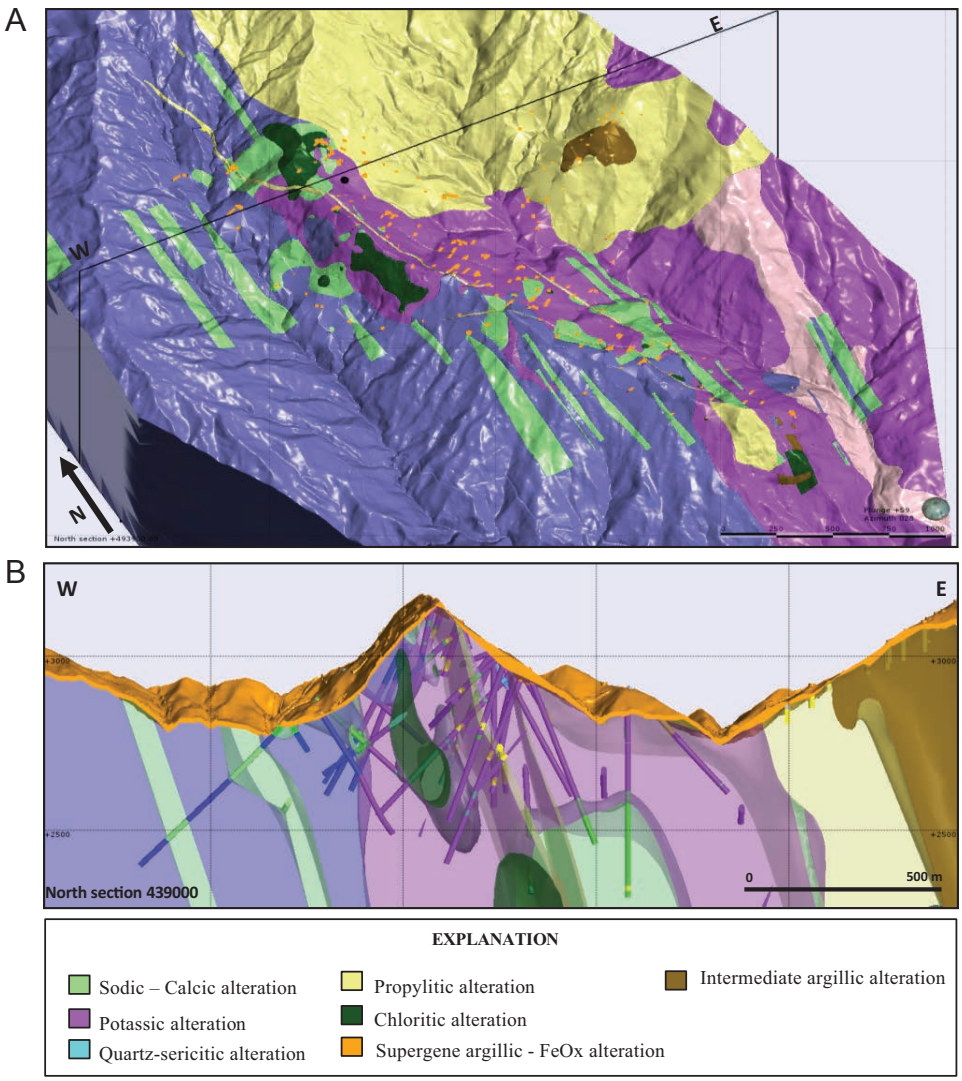

Fig. 8. A. Alteration 3-D model of dominant hydrothermal alteration (excluding supergene argillic Fe oxide) and B. W-E cross section along line 493900 N (looking north) showing the spatial distribution of potassic, sodic-calcic, chloritic, propylitic, intermediate argillic, and supergene argillic Fe oxide hydrothermal alterations at La Colosa porphyry stock (WGS 84 UTM zone, 18N projection).

N-striking corridor of extensional faults, which mainly crosscut the early porphyries, in particular E3. Thus, early potassic alteration in E3 is overprinted by quartz + sericite. The N-striking faults are also locally affected by intermediate argillic alteration.

Sulfide distribution

During visual logging of the drill core the volume fractions of sulfides in the rocks were defined by counting the number of mineral grains visible under the hand lens. The results allowed four 3-D zones of sulfide-oxide enrichment to be distinguished. The first is characterized by 0.2 to 0.5 vol % chalcopyrite, 0.5 to 1 vol % molybdenite, 0.5 to 1 vol % magnetite, and 1 to 2 vol % pyrite associated with early porphyries EDM, EBXDM, and part of E3. The second zone is associated with early porphyries and early intrusive breccias, and it contains 3 to 6 vol % pyrite and 0.2 to 0.5 vol % magnetite. The third zone is characterized by 1 to 3 vol % pyrrhotite and 1 to 2 vol % pyrite in intermineral porphyries and part of the country rock. The fourth zone is characterized by 0.5 to 2 vol % pyrite, 1 to 2 vol % pyrrhotite, and 0.5 to 2 vol % melnikovite in the schistose country rock (Fig. 9).

Veinlets

Nine main veinlet types have been distinguished (Fig. 10) based on their mineralogy, textures, and alteration halos. The typology and nomenclature of the veinlets follows the descriptive criteria for veins and veinlets in porphyry Cu deposits given by Gustafson and Hunt (1975), Sillitoe (2000), and Seedorff et al. (2005). The most common veinlets are A and S types (Fig. 11), as described below.

1. Early biotite (EB) is the earliest veinlet type recognized at the deposit (Lodder et al., 2010). It consists of fine-grained biotite that fills sinuous veinlets (<2 mm wide) associated with the early porphyries (Fig. 10A). No alteration halos are present beside these veinlets.

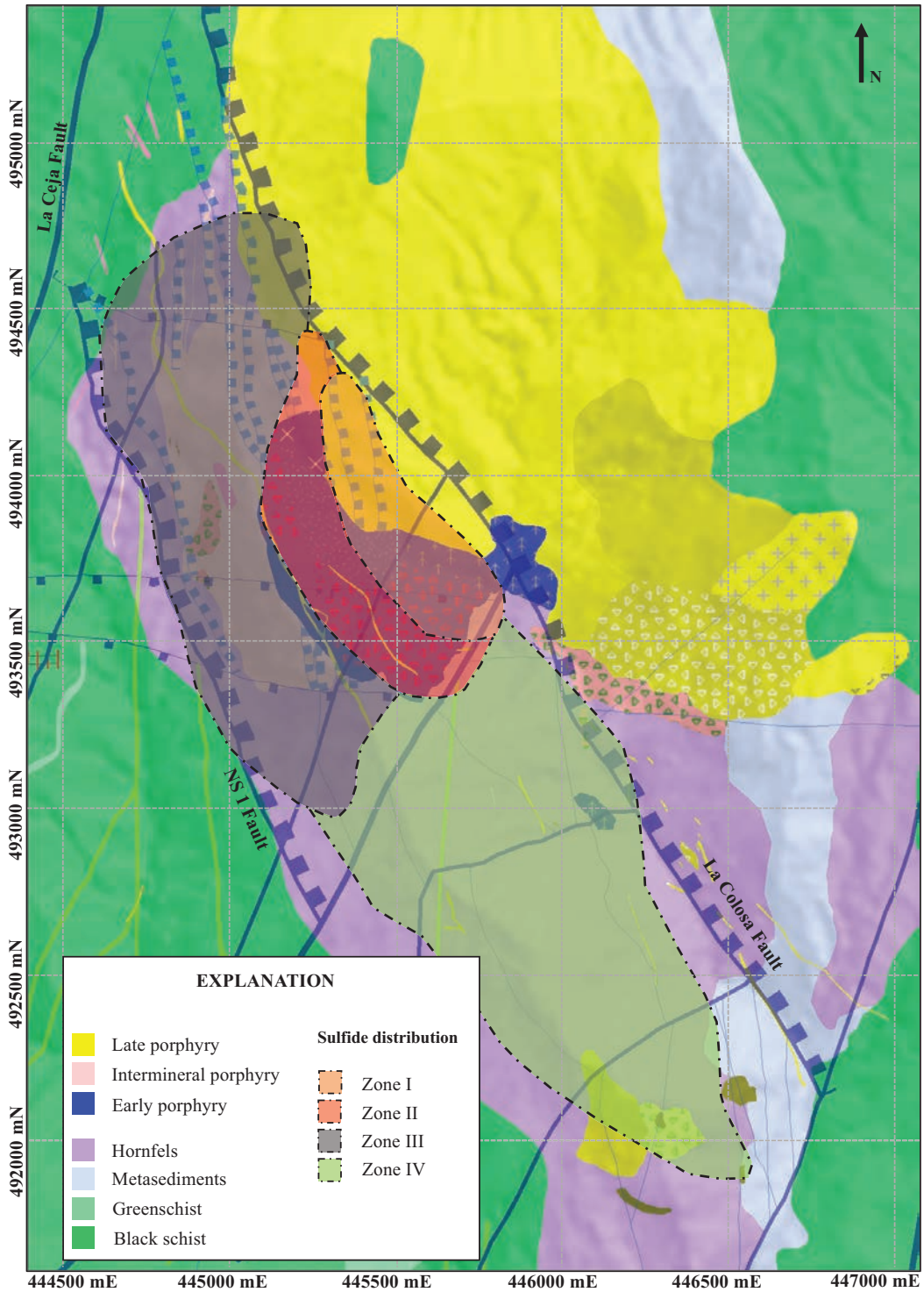

Fig. 9. Simplified geology of La Colosa Au-porphyry deposit and sulfide distribution zones. Zone I: 0.2 to 0.5 vol % chalcopyrite, 0.5 to 1 vol % molybdenite, 0.5 to 1 vol % magnetite, and 1 to 2% vol pyrite, associated with EDM, EBXDM, and part of E3. Zone II: 3 to 6 vol % pyrite and 0.2 to 0.5 vol % magnetite, associated with E0, E1, E2, E3, and early intrusive breccias EBX1 and EBX2. Zone III: 1 to 3 vol % pyrrhotite and 1 to 2 vol % pyrite, associated with intermineral porphyries and schistose country rock. Zone IV: 0.5 to 2 vol % pyrite, 1 to 2 vol % pyrrhotite, and 0.5 to 2 vol % melnikovite, associated with schistose country rock (WGS 84 UTM zone, 18N projection).

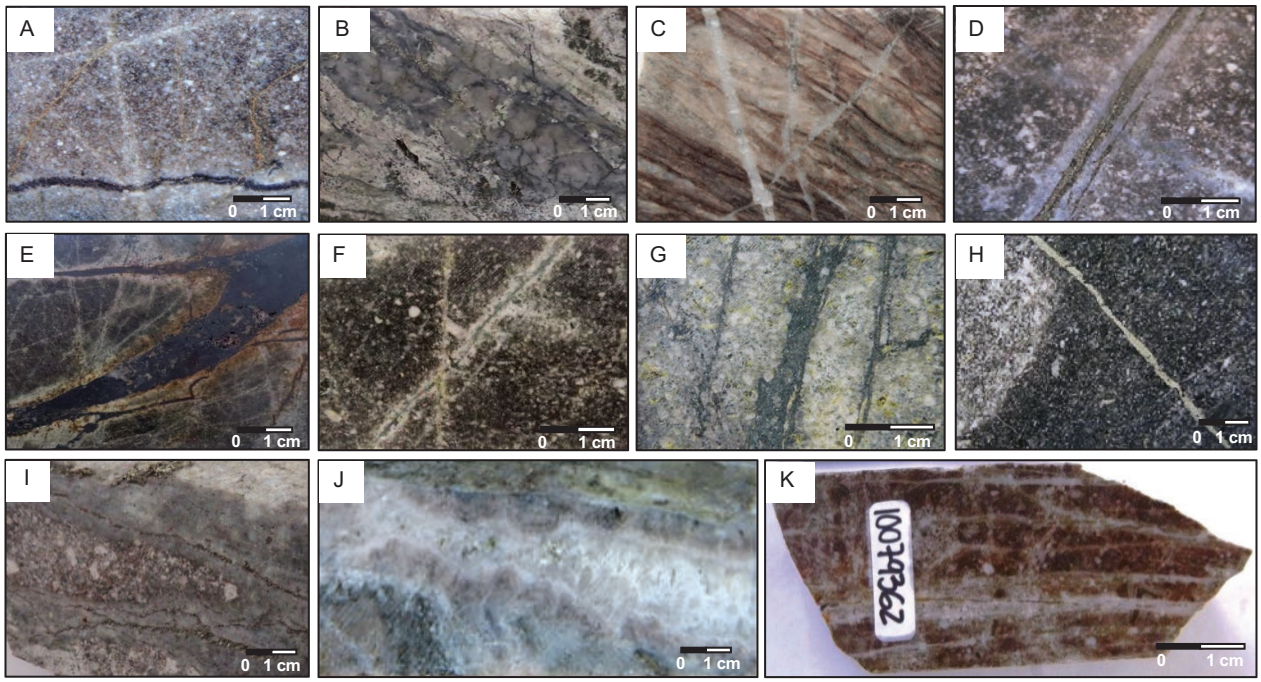

Fig. 10. Photographs of veinlets from La Colosa deposit. A. EB-type veinlets cutting E3 diorite porphyry. B. A-type veinlet with albite halo and disseminated molybdenite. C. A-type veinlets crosscutting schistose wall rock with potassic alteration. D. B-type veinlets with pyrite suture cutting E3 diorite porphyry. E. M-type veinlet with albite halo cutting fine-grained diorite porphyry. F. N-type veinlet forming by albite + actinolite. G. AC-type veinlets crosscutting intermineral breccia IBX with sodic-calcic alteration. H. Pyrite veinlet cutting E3 and fragment of early crowded diorite porphyry E1. I. D-type veinlet composed of pyrite with centimetric quartz-sericitic halo. J. Quartz veinlet with crustiform-colloform texture. K. Sheeted quartz veinlets associated with high-grade mineralization (2 m at 15 g/t Au).

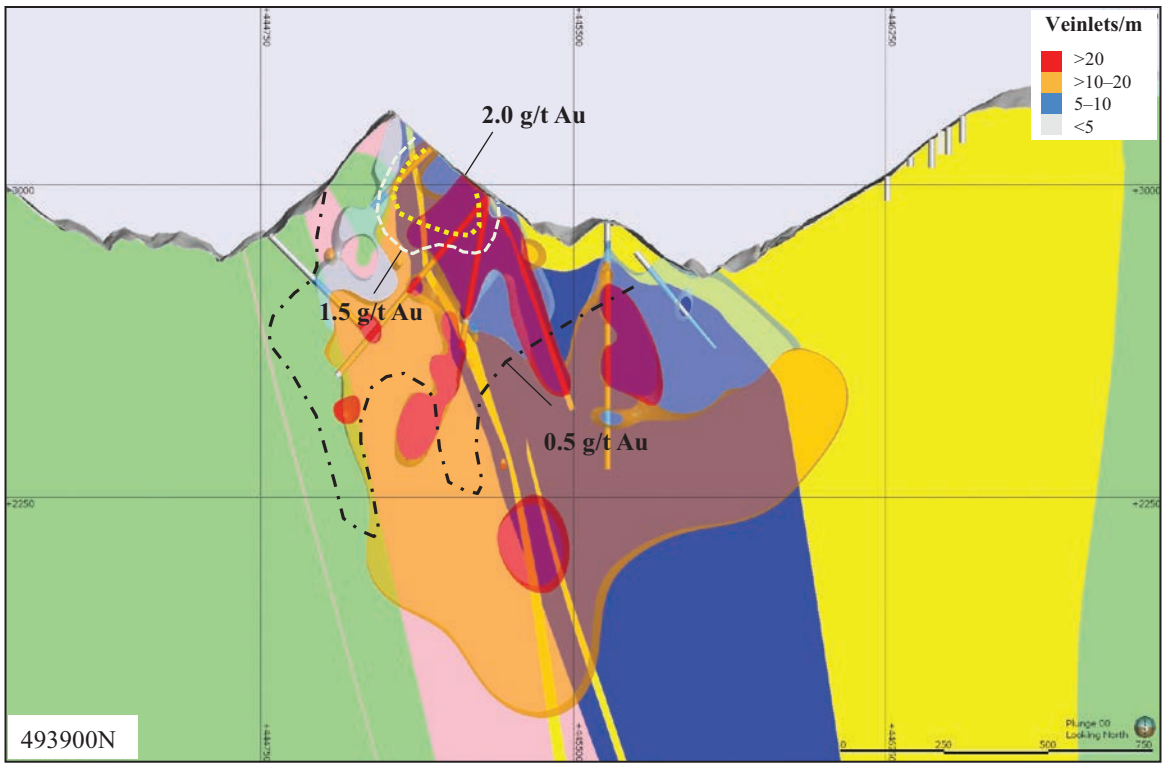

Fig. 11. W-E cross section of veinlet spatial distribution at the La Colosa deposit. Intrusions: early = blue, intermineral = pink, late = yellow, country rocks = pale green. The early porphyry and early intrusive breccias contain the highest concentrations of veinlets, followed by intermineral stage and country rocks, with the lowest concentration of veinlets in the late porphyries. Veinlets/m represents average over 50 m (WGS 84 UTM zone, 18N projection).

2. A-type veinlets are characterized by vitreous or granular quartz along with sulfides, mainly pyrite, pyrrhotite, molybdenite, and chalcopyrite, as well as magnetite. These veinlets (1–10 mm wide) are also sinuous and occur with or without albite ± actinolite alteration halos (Fig. 10B, C). Studies of fluid inclusions (L. Diamond, unpub. report, 2013) show that the quartz precipitated from hypersaline solutions of 40 to 50 wt % NaCl equiv (the inclusions contain daughter crystals of halite and sylvite and accidentally trapped crystals of chalcopyrite and molybdenite). The minimum temperatures of quartz precipitation are set by the homogenization of the inclusions to the liquid phase between 340° and 450°C.
3. B-type veinlets (2–5 mm wide) occur in rectilinear networks and are filled with granular quartz with central sutures lined with pyrite (Fig. 10D); they occur in potassic-altered early and intermineral porphyries, but they are scarce.
4. M-type veinlets (1–5 mm wide) are sinuous or rectilinear and are irregularly filled with magnetite with or without actinolite, K-feldspar, pyrite, molybdenite, and chalcopyrite. Some of these veinlets are bordered by albite + actinolite halos. They occur in all rock types and are spatially associated with the E3 and EDM porphyries in the deep parts of the La Colosa porphyry stock (Fig. 10E).
5. N-type veinlets (1–5 mm wide) are filled with albite accompanied by actinolite and sulfides (Fig. 10F). These rectilinear veinlets are bordered by sodic-calcic alteration, and they occur mainly in the early and intermineral porphyries.
6. Actinolite (AC)-type veinlets (<3 mm wide) are rectilinear, contain traces of pyrite, pyrrhotite, molybdenite, and melnikovite, and are spatially associated with potassic and sodic-calcic alteration in the early and intermineral porphyries and in the schistose wall rocks (Fig. 10G). They show no alteration halos.
7. S-type veinlets (1–5 mm wide) are rectilinear, are dominated by pyrite and pyrrhotite, and occur in all rock types in the La Colosa stock and its country rocks (Fig. 10H).
8. D-type veinlets (1–5 mm wide) are rectilinear, filled by pyrite, and display fine-grained quartz-sericitic halos (Fig. 10I). They are confined to the N-striking dilational corridor.
9. Sheeted quartz veinlets (closely spaced and 1–10 mm wide; Fig. 10K) contain patches of albite + pyrite ± visible gold ± illite ± carbonates, and locally they show crustiform-colloform banding (Fig. 9J). The same mineral assemblage occurs as alteration halos around the veinlets. These rectilinear veinlets are confined to the N-striking dilational corridor. Analyses of fluid inclusions (L. Diamond, unpub. report, 2014) show that the drusy and crustiform quartz precipitated at temperatures between 200° and 350°C from a low-salinity (1.7–4 wt % NaCl equiv) aqueous solution containing traces of CO_2. A second, CO_2-free fluid with high salinity (21–28 wt % NaCl equiv) infiltrated the quartz along microfractures, depositing gold + pyrite + albite + apatite + anatase between 150° and 200°C. Residual cavities in the veinlets were subsequently filled by calcite. Other minor veinlet types distinguished at La Colosa are monomineralic K-feldspar, chlorite, and gypsum.

Mineralization and Metal Zoning

Contours of metal concentrations (Au, Cu, Mo, Ag) were fitted to the drill core database using Leapfrog software. The database contains 65,572 samples analyzed for gold by fire assay and by ICP for trace elements, retrieved from 138,696 m of drilling. Surface samples have been included to constrain the fits of the contours. The dispositions of the resulting 3-D isosurfaces of average metal contents (hereafter termed "shells") reveal correlations between ore and host rock types, contacts, hydrothermal alteration, vein types, and brittle structures.

Gold

Metallurgical and geometallurgical studies on composited and selective samples indicate that gold occurs predominantly as native gold, as electrum, and in minor quantities as gold tellurides and gold-silver tellurides (Leichliter, 2013). Gold occurs as isolated grains and as inclusions or fracture fillings in pyrite, pyrrhotite, and silicate minerals such as feldspar and quartz (Fig. 12).

Three gold mineralization events have been recognized at La Colosa. The first is associated with the various porphyry phases of the intrusive complex (Fig. 13A, B). The early porphyries and early intrusion breccias have gold ranging in grade from 0.75 to 1.0 Au g/t. Veinlets of A and S type are abundant, and potassic alteration is common. The gold grade of the intermineral porphyries and breccias is lower, from 0.5 to 0.75 Au g/t. In the late-stage porphyries, gold grade drops to <0.3 Au g/t. In this first event, gold was concentrated at the contact zone between the intrusions and their country rocks and also in fracture zones that follow the NNW- to N-trending D_1 folds in the country rocks. These zones can be traced through the schistose basement rocks for 1 km north and south of La Colosa porphyry stock.

The second gold event was focused within the N-striking extensional faults that crosscut the early, intermineral, and late-stage porphyries as well as the country rocks. Sheeted quartz veinlets are abundant, and they contain quartz and pyrite with centimeter-wide halos of albite + sericite ± carbonate (Fig. 12D). In the late tonalite porphyry, this second event is represented by sparsely distributed pyrite ± sericite veinlets (<3 per m in drill core) with elevated gold grades (>1 g/t Au; Fig. 12). At La Colosa these high-grade sheeted quartz veinlets occur along the strike of the faults for hundreds of meters into the northern part of the deposit, and their extent remains open for further exploration. The third gold event was a local product of supergene enrichment in the late tonalite and quartz diorite porphyries due to weathering that produced clays and iron oxides (Fig. 13A). Thus, the gold grade is enriched from 0.1 Au g/t in unaltered rocks to 1.5 Au g/t in weathered rocks.

Gold-grade shells

The grade shells for 0.5, 1.5, and 2.0 g/t Au illustrate the distribution of gold within the deposit (Fig. 13A, B; Digital App. 1). The 0.5 g/t Au shell encompasses early and intermineral intrusions and some portions of the schistose country rock. In detail, three separate zones can be recognized within this shell. The first shows grades between 0.5 and 0.7 g/t Au and is associated with porphyries E3 and EDM and the breccia EBXDM.

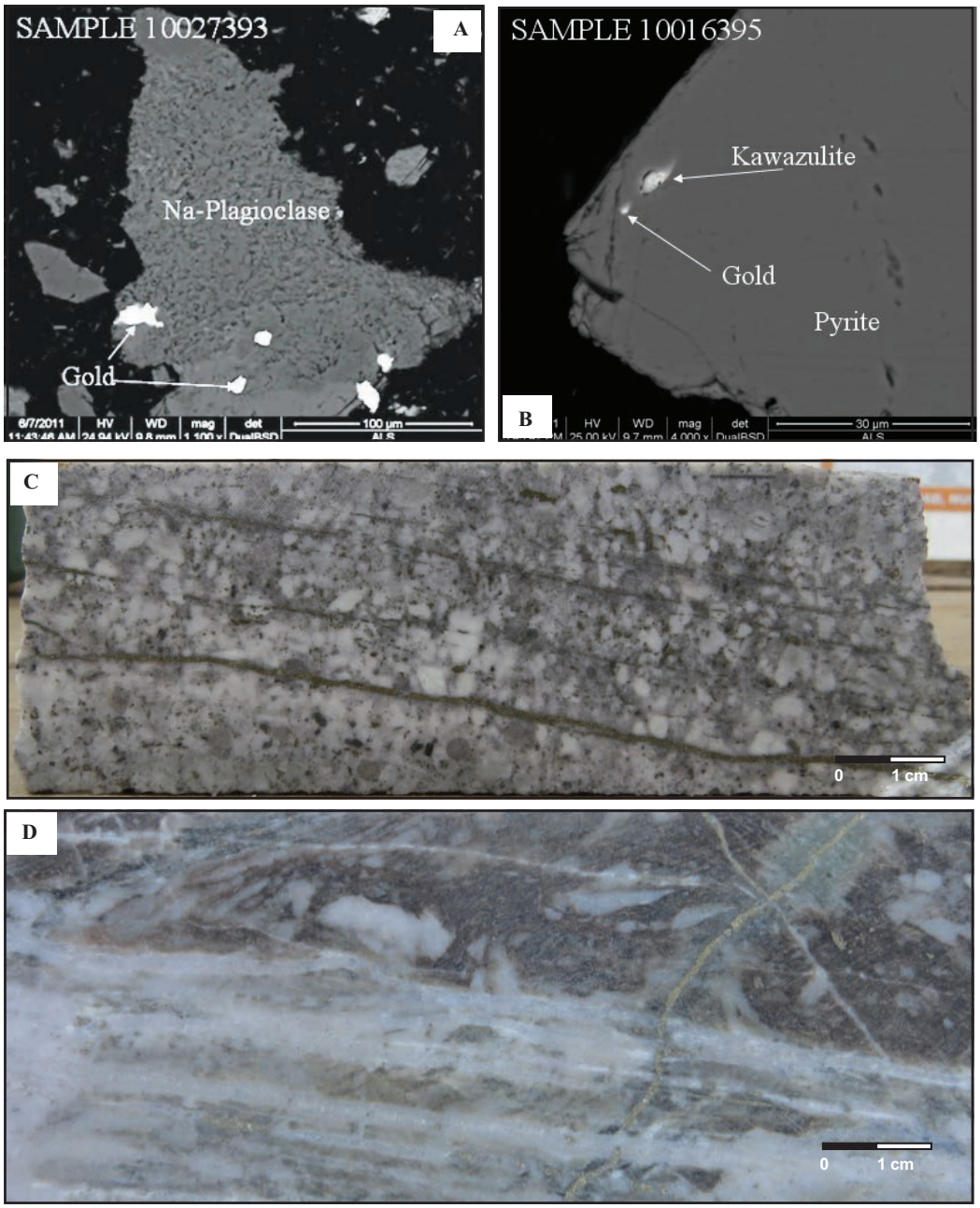

Fig. 12. Photographs of gold occurrences and sheeted veinlets at La Colosa Au-porphyry deposit. A-B. Mineral liberation analysis, backscattered electron images of gold occurrences. C. Sheeted pyrite veinlets with centimeter-wide sericite halo cutting coarse-grained tonalite porphyry, containing 1,082 ppm Au over 2 m. D. Sheeted quartz veinlets with sericite halos hosted by country rock, containing 9,270 ppm Au over 2 m.

All of these rocks exhibit potassic alteration and contain A- and M-type veinlets with pyrite, chalcopyrite, and molybdenite. This first gold zone partly overlaps with a grade shell that contains the highest values of copper (>0.1%), molybdenum (>0.01%), and silver (>1 g/t) at La Colosa (Fig. 13A).

The second zone within the 0.5 g/t Au shell (Fig. 13A) is hosted by early porphyries (E0, E1, E2, and E3) and breccias (EBX1 and EBX2) and a portion of intermineral porphyries. Disseminated pyrite is the dominant sulfide. A-, S-, and D-type veinlets occur within the zone and contain uncommon magnetite, chalcopyrite, molybdenite, and K-feldspar. The gold ranges in grade from 0.75 to 1 g/t Au. The third zone is marked where the abundance of pyrrhotite exceeds that of pyrite (Fig. 13A). In this zone intermineral porphyries and intermineral intrusion breccias predominate, showing potassic and subordinate chloritic alteration, which is dominant in the central part of the intermineral porphyry where the gold grade drops from 0.7 to 0.5 g/t Au.

Part of the gold in the 0.5 g/t Au shell (Figs. 4, 13A) is hosted by the hornfelsed schistose country rock, which shows silicification, potassic, and sodic-calcic alteration, and which contains A- and S-type veinlets with pyrrhotite, pyrite, and

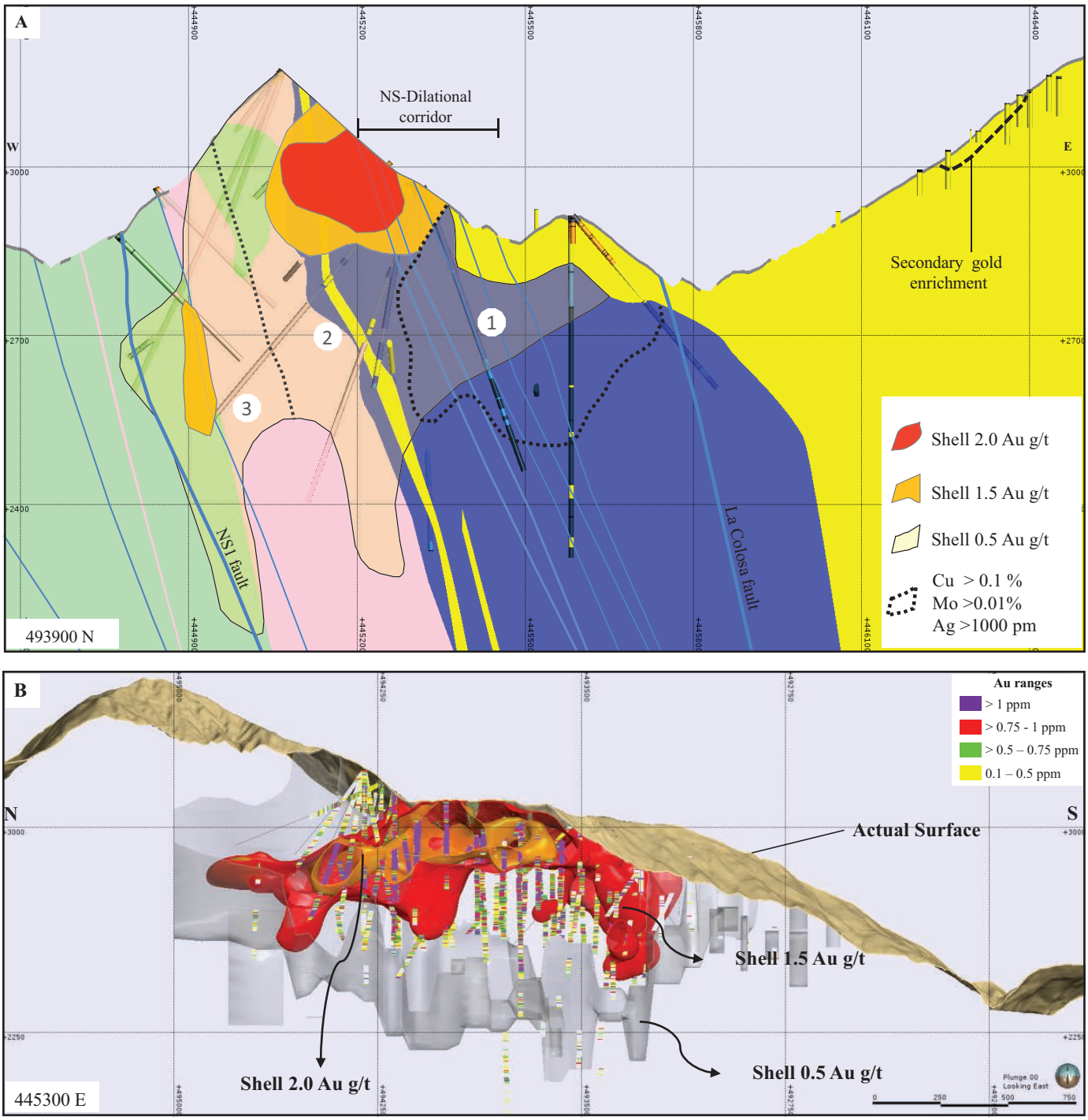

Fig. 13. Cross sections of gold shells within the La Colosa deposit. A.W-E cross section along line 493900 N showing early, intermineral, and late porphyries, faults, and mineralized shells of gold, copper, molybdenum, and silver. 1 = gold area overlapping shell of copper, molybdenum, and silver, 2 = gold area with pyrite as the dominant sulfide, A-, S-, and D-type veinlets, and uncommon magnetite, chalcopyrite, molybdenite, and K-feldspar, 3 = gold area marked by pyrrhotite as dominant sulfide. Section thickness 100 m (WGS 84 UTM zone, 18N projection). B. N-S cross section along line 445300 E showing 0.5 g/t Au (gray), 1.5 g/t Au (red), and 2.0 g/t Au (orange) gold shell, and resource drill holes with Au ranges. Section thickness 300 m (WGS 84 UTM zone, 18N projection).

melnikovite. In total, the 0.5 g/t Au shell contains 1,107 Mt of ore with 684 t (22 Moz) of gold, averaging 0.62 g/t.

The grade shells for 1.5 and 2.0 g/t Au (Fig. 13A, B) are hosted by early, intermineral, and late porphyries and intrusion breccias, as well as country rock. The 1.5-g/t Au shell extends over 1.2 km of surface length and contains 196 Mt of ore with 271 t Au (8.7 Moz) at 1.38 g/t Au whereas the 2.0 g/t Au shell covers 0.75 km and contains 40.7 Mt of ore with 84 t Au (2.7 Moz) at 2.04 g/t Au.

Deep copper, molybdenum, and silver zone

Copper, molybdenum, and silver are closely associated in space, and their highest grades are found in the eastern part of the deposit between 2,400 and 2,600 m a.s.l. (Fig. 13A). Average grades are 0.11 wt % Cu, 0.017 wt % Mo, and 2.3 g/t Ag.

Geochronology

Fifty-five samples from La Colosa deposit and adjacent porphyry stocks were selected for radiometric age dating using the U-Pb, Re-Os, and K-Ar methods (Table 1; Fig. 14). Sample preparation and analysis were carried out at VU Geoservices Corporation (Arizona).

U-Pb analyses were used to date the crystallization ages of the La Colosa porphyry stock and its adjacent intrusive centers, as well as to obtain information on the maximum deposition age of the schistose country rocks. Re-Os dating was used

Table 1. Summary of Geochronology Samples at La Colosa Deposit and Adjacent Porphyries

Method	E	N	Location	Rock	Age (Ma)	Error + (Ma)	Error – (Ma)
U-Pb	445188	494112	Colosa	TO	7.9	0.3	0.3
U-Pb	445267	493890	Colosa	TO	7.6	0.2	0.2
U-Pb	445389.9	493142.7	Colosa	TO	7.8	0.1	0.1
U-Pb	445827	493197.5	Colosa	TO	7.6	0.1	0.2
U-Pb	445991.7	492608.3	Colosa	TO	7.8	0.1	0.1
U-Pb	445499.4	494271.5	Colosa	TO	8.2	0.1	0.1
U-Pb	445188.9	493721.4	Colosa	TO	8.2	0.2	0.1
U-Pb	445323.5	493732.4	Colosa	TO	7.4	1	1
U-Pb	445527.8	493504.9	Colosa	TO	7.4	0.1	0.1
U-Pb	446113.7	493783.1	Colosa	QZDI	8	0.1	0.1
U-Pb	445284.7	494188.4	Colosa	E0	8.4	0.1	0.2
U-Pb	445188	494112	Colosa	E1	8.3	0.2	0.2
U-Pb	445287.7	493864.9	Colosa	E3	8.5	0.3	0.1
U-Pb	445274.5	494107.9	Colosa	EBX1	8.3	0.2	0.1
U-Pb	445270.5	493864.1	Colosa	EBX2	8.2	0.1	0.1
U-Pb	445876.5	493808	Colosa	EDM	8.4	0.2	0.2
U-Pb	445400.9	493204.8	Colosa	I1	8.4	0.1	0.2
U-Pb	444709.6	495045.4	Colosa	I1	8.4	0.1	0.1
U-Pb	445023	493787.5	Colosa	I2	8.3	0.1	0.1
U-Pb	445567.3	492702.2	Colosa	I2	8.4	0.1	0.2
U-Pb	445790.6	492499	Colosa	I2	8.3	0.1	0.1
U-Pb	444952.4	494110	Colosa	IBX	8.2	0.2	0.2
U-Pb	445400	501010	El Delirio	QZDI	8.2	0.3	0.2
U-Pb	450141	493903	La Bolivar	TO	7.4	0.2	0.1
U-Pb	450764	493532	La Bolivar	QZDI	7.7	0.2	0.1
U-Pb	448425	494335	La Bolivar	TO	7.6	0.1	0.2
U-Pb	442840	501174	El Tabor	QZDI	7.2	0.2	0.1
U-Pb	450560	508340	Dantas	DI	6.3	0.1	0.1
U-Pb	443103.6	496942.2	La Oscurana	TO	7.2	0.3	0.1
U-Pb	446232.2	492110.3	San Antonio	IS2	8.4	0.2	0.1
U-Pb	446255.6	492046.7	San Antonio	LS	8	0.1	0.1
U-Pb	446355.2	492071.4	San Antonio	SABX	8.3	0.1	0.1
U-Pb	442622	493688	Sincelejo	DI	8.3	0.1	0.1
U-Pb	442278	493771	Sincelejo	QZDI	8.3	0.1	0.1
U-Pb	442032	491678	La Linea tunnel	DI	8.3	0.1	0.2
U-Pb	438829	492205	14C	DI	8.2	0.1	0.1
U-Pb	442840	501174	Montecristo	QZDI	7.6	0.2	0.2
U-Pb	446453	505276	Tierradentro	DI	8.1	0.1	0.1
U-Pb	438324	511164	Salento	GRDI	6.3	0.3	0.3
U-Pb	440322	504063	La Morena	DI	8.4	0.2	0.2
U-Pb	449982	482013	California	QZDI	3.4	0.2	0.1
K-Ar	445600	493400	Colosa	EBX1	7.9	0.8	0.8
K-Ar	444960	492930	Colosa	IBX	8	0.8	0.8
Re-Os	445611	492993	Colosa	H	8.24	0.08	0.08
Re-Os	445230	493861	Colosa	EBX2	8.18	0.06	0.06
Re-Os	446361	492993	Colosa	H	3.24	0.06	0.06

WGS 84 UTM, 18N projection

Abbreviations: DI = diorite porphyry, E0-E1-E3-EDM = early porphyries, EBX1-EBX2 = early intrusive breccias, GRDI = granodiorite porphyry, H = hornfels, I1-I2 = intermineral porphyries, IBX = intermineral intrusive breccia, IS2-LS = late porphyries, QZDI = quartz diorite porphyry, SABX = intrusive breccia, TO = tonalite porphyry

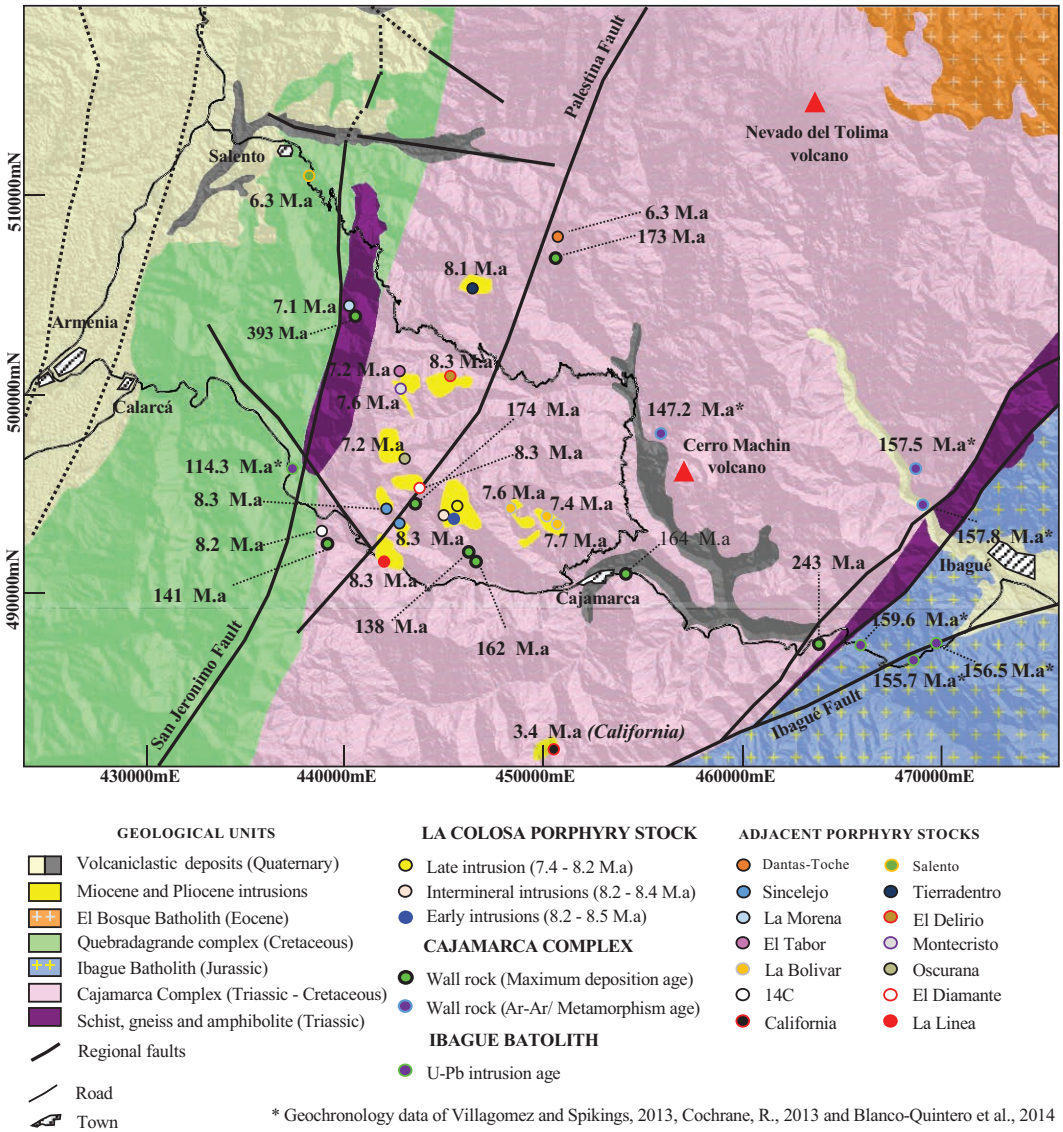

Fig. 14. Simplified regional geology and location of radiometric ages (WGS 84 UTM zone, 18N projection).

to constrain ages of the mineralization, and K-Ar dating was used to determine cooling ages and constrain hydrothermal alteration events.

U-Pb ages

Heavy mineral concentrates of the <350-μm fraction were separated using conventional techniques at ZirChron LLC. Zircons from the nonmagnetic fraction were mounted in epoxy and slightly ground and polished to expose the surface and keep as much material as possible for laser ablation analyses. Cathodoluminescence images were acquired to guide the analyses. Spots on the zircons were analyzed using a New Wave Nd:YAG UV 213-nm laser (30-μm spot size and 10 Hz) coupled to a ThermoFinnigan Element 2 single collector, double-focusing, magnetic sector inductively coupled plasma-mass spectrometer (ICP-MS). Each analysis consisted of a short blank analysis followed by 250 sweeps through masses 204, 206, 207, 208, 232, 235, and 238, taking approximately 30 s. Time-independent fractionation was corrected by normalizing U/Pb and Pb/Pb ratios of the unknowns to the zircon standards. For this study, two zircon standards were used: Peixe, with an age of 564 Ma, and FC-1, with an age of 1099 Ma. Uranium-lead ages and errors (2σ) were calculated using Isoplot® (Ludwig, 2012), a geochronological toolkit for Microsoft Excel.

La Colosa district intrusive rocks

The U-Pb ages of the La Colosa porphyry stock (Figs. 14, 15A, B) are between 7.4 and 8.5 Ma. These ages indicate the early, intermineral, and late stages at La Colosa were emplaced during a short time span of ~1.1 ± 0.2 m.y. The adjacent porphyry stocks (within a 10-km radius of La Colosa) returned ages between 6.3 and 8.4 Ma (Figs. 14, 15A), defining a magmatic cluster. The stock at the California prospect ~7 km southeast of La Colosa (Figs. 14, 15A) was dated at 3.4 Ma and thus represents a younger magmatic event in the area, which

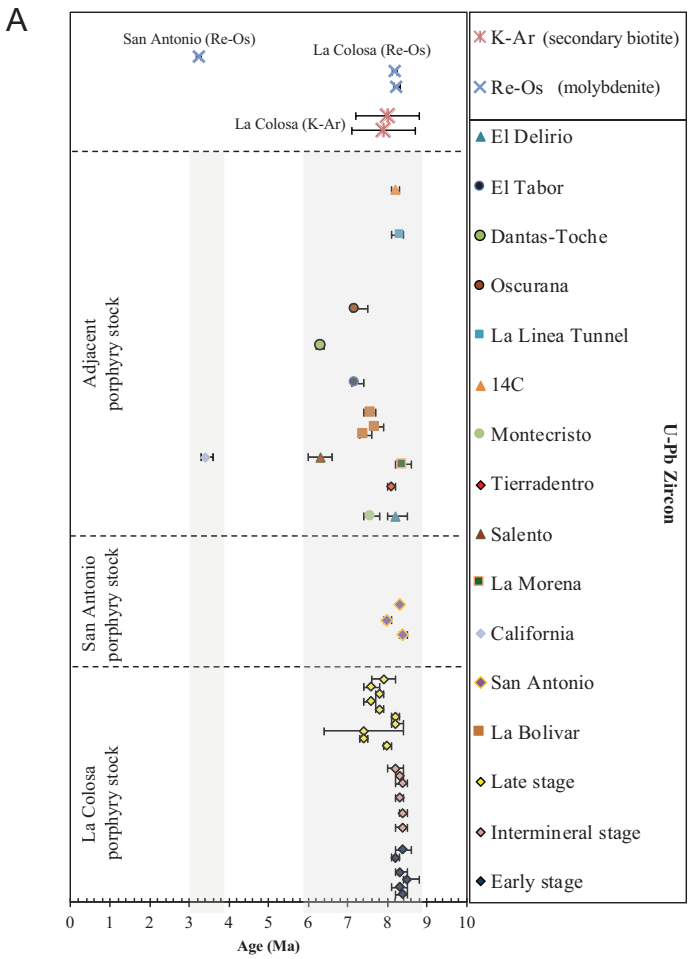

Fig. 15. A. Summary of radiometric ages of La Colosa deposit and adjacent porphyry stock (U-Pb, K-Ar, and Re-Os). B. Concordia plots for zircon U-Pb analyses, La Colosa Au porphyry deposit. Porphyry stages: early stage (10050654), intermineral stage (10076894), late stage (10110612). Wall rocks: metasediment (12072894) and hornfels (12079841) (V. Valencia, unpub. report, 2015).

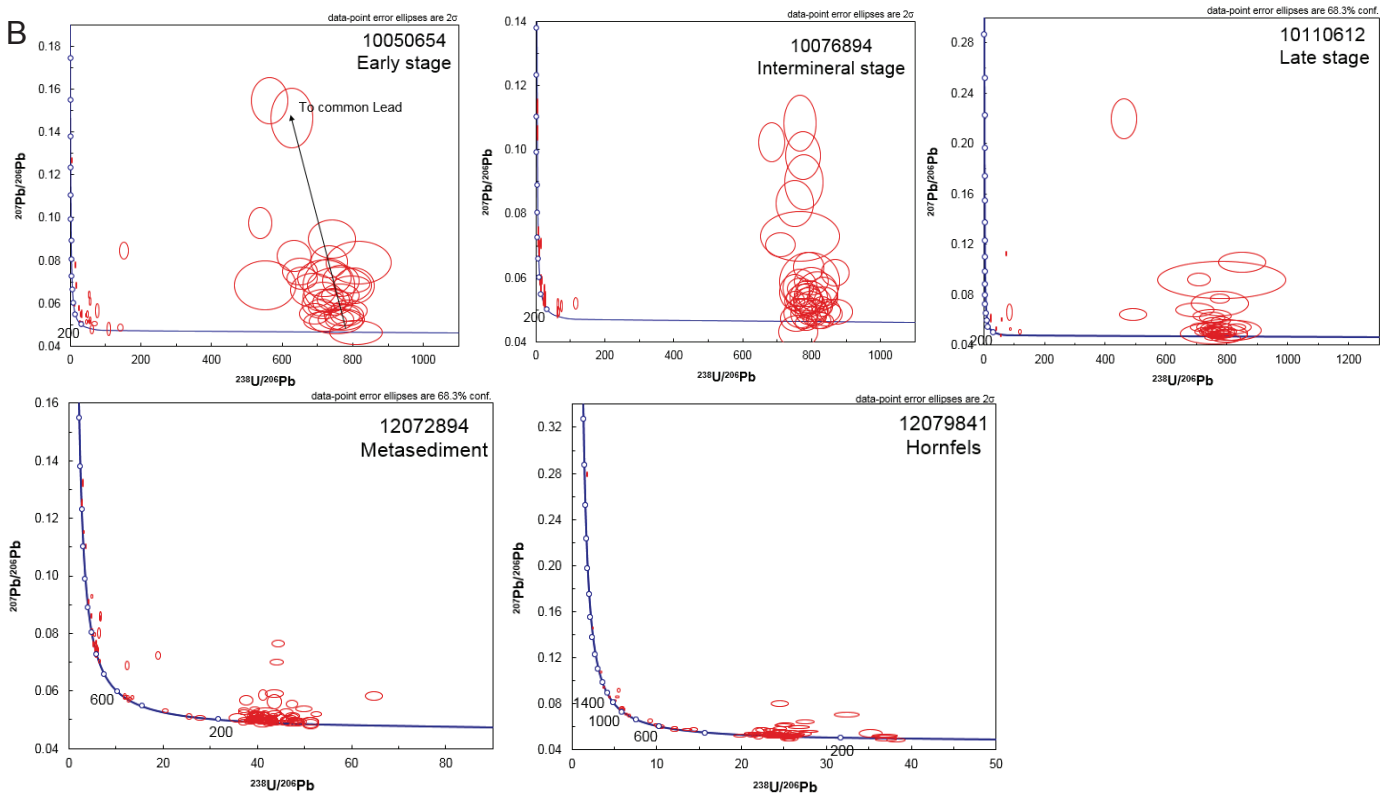

correlates with the Pliocene to Recent volcanic activity of the Northern volcanic zone (Digital App. 2).

Re-Os and K-Ar ages

Molybdenite was dated by the Re-Os method, with all sample preparation and analyses carried out at the University of Arizona. Approximately 0.5 g of Re-Os spikes were loaded and digested using the Carius tube method. The tube was placed in an oven and heated to 240°C for 24 h. Rhenium and Os were separated using the distillation technique, in which the Os is collected into cold HBr, dried down, and redissolved in 0.1 HNO_3. Rhenium was extracted using AG1-X8 anion exchange column chemistry. Rhenium and Os were later loaded on Ni and Pt filaments, respectively, with Ba salts to enhance ionization. Measurements were made using the negative thermal ion mass spectrometer (NTIMS).

The Re-Os ages of molybdenite indicate that mineralization occurred during two distinct periods (Table 2). The first was simultaneous with the emplacement of the early, intermineral, and late porphyries of La Colosa stock (8.24 ± 0.08–8.18 ± 0.06 Ma). The second period was dated at 3.24 ± 0.06 Ma at the San Antonio porphyry stock.

In order to constrain the age of hydrothermal alteration at La Colosa stock, two samples of the early porphyries with pervasive hydrothermal biotite alteration were analyzed by the K-Ar method, yielding cooling ages of 8.0 ± 0.8 and 7.9 ± 0.8 Ma (Leal-Mejia, 2011; Table 1; Fig. 15A).

Zircon ages in country rocks

Detrital zircons in eight samples of schistose country rock from the Cajamarca Complex were analyzed by the U-Pb method (Table 3; Fig. 14). Several zircon populations were identified, with major peaks at 255 to 99, ~600 to 400, and ~1200 to 1000 Ma. The ages indicate several sources of detrital zircons. In addition, the age populations constrain the maximum age of deposition of the Cajamarca Complex to between ~243 and ~99 Ma (Early Triassic to beginning of Late Cretaceous) (Digital App. 3, 4).

Discussion

Age and deformation of the country rocks

The new radiometric dating and structural results presented in this study allow the age and deformation history of the country rocks at La Colosa, the Cajamarca Complex, to be better defined. According to Vargas et al. (2005), the basement of the Cajamarca Complex is Devonian gneiss (~393 Ma). Based on $^{40}Ar/^{39}Ar$ dating of metapelites and amphibolites of the Cajamarca Complex close to La Colosa, a Late Jurassic metamorphic event was suggested by Blanco-Quintero et al. (2014). This Late Jurassic event correlates with crystallization ages between 159.6 and 155.7 Ma for the Ibagué batholith obtained by Villagómez et al. (2011) and Cochrane (2013). U-Pb detrital zircon ages obtained in the present study vary from 243 to ~99 Ma. The oldest deposition ages of the Cajamarca Complex are Triassic and have been identified in its eastern part near the Ibagué batholith. Radiometric ages gradually pass to Jurassic (174–162 Ma) at the latitude of the town of Cajamarca. In the western areas close to the crest of the Central Cordillera (La Línea ridge) the youngest ages have been found from 138 to 99 Ma. Although the Romeral fault system, with the San Jeronimo fault as its easternmost branch, marks the boundary between the Cajamarca Complex to the east and the Quebradagrande Complex to the west, the exact location of this boundary is not well defined. The ages of the Quebradagrande Complex vary from Barremian to Albian (Moreno-Sanchez et al., 2003; Nivia et al., 2006; Blanco-Quintero et al., 2014), similar to the detrital zircon age in the western part of Cajamarca Complex. The gradual decrease in the age of the Cajamarca Complex toward the Quebradagrande Complex to the west indicates that both complexes may have had a similar origin but a different metamorphic history and extent of exhumation.

The deformation event D_1 that affects the Cajamarca Complex may be associated with the main regional metamorphism and the onset of the Andean orogeny in the Late Cretaceous to Paleocene (e.g., Nie et al., 2010; Parra et al.,

Table 2. Re-Os Data for La Colosa and San Antonio Porphyry Stocks

Sample ID	Stock	^{187}Os (ppb)	^{87}Re (ppm)	Age (Ma)	Error (Ma)	Lab
10070010	San Antonio	0.49	8.98	3.24	0.02	VUGCP
10070304	La Colosa	50.15	365.31	8.24	0.06	VUGCP
10050749	La Colosa	51.79	381.93	8.18	0.06	VUGCP

Abbreviations: VUGCP = VU Geoservices Corporation, Tucson, Arizona

Table 3. Summary of U-Pb Ages of Maximum Deposition of the Schistose Country Rock, Cajamarca Complex

Method	E	N	Location	Sample no.	Rock	Maximum deposition age (Ma)
U-Pb	446531.18	491758.29	Colosa	12072893	Hornfels	162
U-Pb	446596.49	492027.25	Colosa	12072894	Metasediments	138
U-Pb	443704.00	494683.00	Diamante	12072892	Black Schist	174
U-Pb	454233.11	491069.45	Cajamarca bridge	12079448	Greenschist	164
U-Pb	463763.82	487640.67	Perico-Cajones bridge	12079449	Black schist	243
U-Pb	450610	507111	Dantas-Toche	12079841	Hornfels	173
U-Pb	440509	504004	La Morena	12079881	Gneiss	393
U-Pb	439146	492675	La Linea	12079893	Chert	141

WGS 84 UTM, 18N projection

2012). Alternatively, it may be correlated with an earlier, probably Late Jurassic metamorphic event, as suggested by Blanco-Quintero et al. (2014). The D_2 ductile deformation may, therefore, reflect the later Andean deformation marked by thrusting of the Cajamarca Complex onto the accreted terranes to the west as a result of the collision of the South American margin with the Caribbean large igneous province during the Late Cretaceous-Paleocene (Villagómez et al., 2011; Spikings et al., 2015).

Structural controls on magmatism and hydrothermal activity

The local field observations made in this study and those made at the regional scales by other workers provide insight into the development of structures that focused magmatic activity at the La Colosa site. The regionally extensive, NNE-striking Palestina fault system, which hosts the deposit, may have originated as a ductile, deep-seated shear zone that evolved to a fault system with brittle characteristics. Some workers have attributed right-lateral displacement to the Palestina system (e.g., Cediel et al., 2003; Mora-Bohórquez et al., 2017). However, global positioning system (GPS) data (Kellogg and Vega, 1995), fault kinematic studies (Ego et al., 1996; Acosta et al., 2004; Cortés et al., 2006), and analyses of seismic data (Taboada et al., 2000; Corredor, 2003; Cortés and Angelier, 2005) have suggested that the shear direction along the Palestina and other regional fault systems, such as the Romeral fault (Figs. 2, 16), has changed from right-lateral to left-lateral since the mid-Miocene. The trigger for this change is thought to have been the interaction of the South American plate with the E-migrating Caribbean plate and the docking of the Panamá-Chocó block. This modified the Miocene stress field north of latitude 4–5° N, inducing WNW- to NW-directed compression and thereby reversing shear along the regional fault systems.

A consequence of this reversal of stress orientation was the formation of secondary faults, such as N-striking synthetic Riedel shear structures (R), some of which seem to have followed inherited anisotropy within the metamorphic basement rocks, such as the D_1 ductile shear zones. NW- to W-trending faults were also generated, interpreted here as antithetic Riedel shear faults (R'), as indicated by their slight right-lateral senses of movement. Subsequent movement along the regional faults developed N- to NW-striking extensional faults, indicating extension in east-west to southwest-northeast direction. This promoted linkage of several faults in between the major strike-slip faults, generating local pull-apart structures and thus creating extensional centers into which the La Colosa and San Antonio stocks intruded (Fig. 3). The NW-trending contact between the early and the intermineral porphyries and the NW-trending tonalitic dikes (Fig. 4) reflects the stress regime with NE-SW–directed extension, which acted during the emplacement of the magmatic stock at La Colosa. The emplacement of the La Colosa and San Antonio intrusive stocks is, consequently, associated with and delimited by pull-apart structures controlled by the regional NE-trending strike-slip fault system.

Whereas the Palestina fault system clearly controls the longitude of the La Colosa and San Antonio stocks, another large-scale tectonic feature may have influenced the latitude of their host pull-apart structures. According to the interpretation of current seismicity data, a W-trending tear zone (Caldas tear) associated with the subducting slab of the Nazca plate has been proposed by Vargas and Mann (2013). This tear zone extends for approximately 240 km in an east-west direction at about 5° N and is colinear with a now-extinct, ~9 to 12 Ma oceanic spreading ridge. Furthermore, this tear structure is the likely boundary between two different subducted slabs having different dips. It may, therefore, have played a role in localizing the La Colosa deposit.

Following the intrusive activity at La Colosa and San Antonio, uplift and progressive deformation along the regional structures continued to develop the N- and NW-striking normal faults within the local pull-apart structures. These extensional faults crosscut the porphyries as well as the metamorphic basement rocks and acted as conduits for the late hydrothermal fluids that precipitated the high-grade, sheeted quartz-pyrite Au veinlets (Figs. 3, 12). Although deformation along the major structures continued during this period of postporphyry emplacement, other fault orientations, including the contact zones of the pull-apart structure, were unfavorable for the deposition of high-grade mineralization.

Hydrothermal alteration and mineralization at La Colosa

Whereas the U-Pb ages at La Colosa show that the composite porphyry stock was emplaced between 8.5 and 7.4 Ma, the Re-Os ages for molybdenite show that mineralization occurred at ~8.2 Ma, simultaneous with emplacement of the early, intermineral, and late porphyry stocks (8.24 ± 0.08–8.18 ± 0.06 Ma). The K-Ar closure ages of secondary biotite indicate that the deposit passed through approximately 300° to 400°C soon thereafter, at 8.0 ± 0.8 Ma. The entire intrusive and hydrothermal mineralization events thus occurred within a relatively short, ~1.1 m.y. time interval. However, Re-Os ages for molybdenite at the San Antonio porphyry stock show that mineralization there occurred significantly later, at ~3.24 Ma. Evidently, the hydrothermal systems at the two magmatic centers are unrelated to each other.

Gold deposition at La Colosa was primarily controlled by the sequence of intrusions. The early porphyries carry the highest gold grades (0.75–1.0 g/t Au), then the intermineral porphyries follow with intermediate grades (0.5–0.75 g/t Au), and finally the late porphyries have the lowest grades (<0.3 g/t Au). Part of the gold mineralization is hosted by the country rock adjacent to the mineralized stocks. Most of the gold is situated in A- and S-type veinlets with pyrite as the dominant sulfide, accompanied by potassic alteration. The best-developed Cu-Mo-Ag mineralization is associated with early porphyries and breccias (E3, EDM, and EBXDM) deep in the deposit, but total tonnages are subeconomic. Although this zone overlaps with some of the gold-rich zones, its geometry and depth suggest that Cu, Mo, and Ag are basically decoupled from gold. Overall, many features of the mineralization at La Colosa, including the porphyritic rock textures, the range of hydrothermal alteration assemblages and veinlet types, and the relatively short time interval (~1.1 m.y.) during which the stocks were emplaced are quite typical of Au porphyry deposits elsewhere (e.g., Sillitoe, 2000).

A more unusual and economically key feature at La Colosa is the occurrence of a significant portion of the total gold

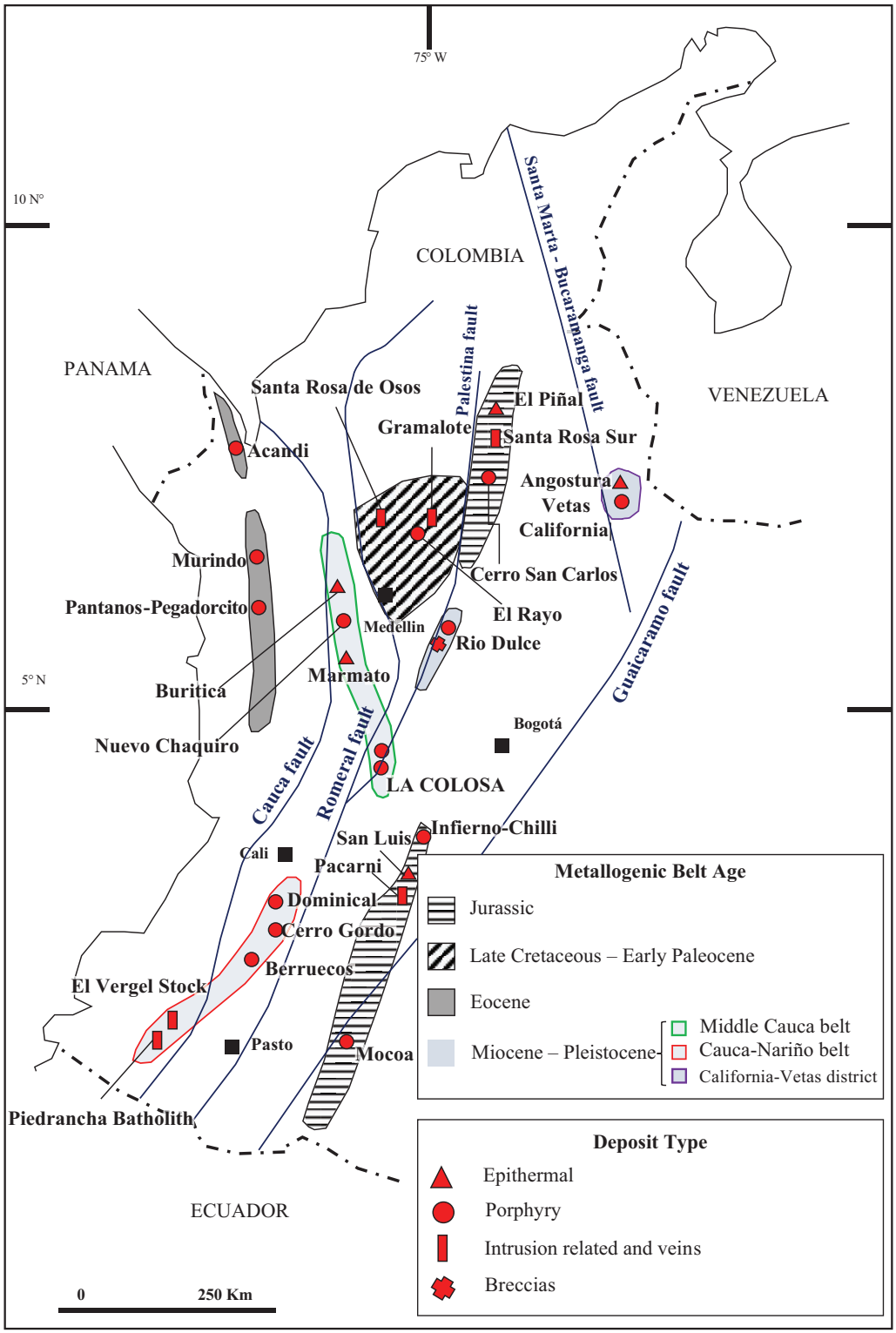

Fig. 16. Magmatic and mineralized belts of Colombia, showing known gold deposits. Modified from Sillitoe (2008) and Leal-Mejia (2011).

resource (~8 Moz) in late extensional faults that crosscut the intrusive complex and strike northward far into the surrounding country rocks. The sheeted quartz-pyrite veinlets that contain the high-grade gold (>1.5 g/t) in this structural corridor are accompanied by sericite + albite alteration rather than by the dominantly potassic alteration characteristic of the earlier porphyry-stage mineralization. Presumably the sheeted quartz-pyrite veinlets formed from fluids that evolved from a parent magma chamber well below the level of the drilled stocks.

Mineralized magmatic belts of Colombia

Several metallogenic belts have been defined as a function of the tectonomagmatic evolution of the northern Andes (Sillitoe et al., 1982; Rodríguez and Warden, 1993; Sillitoe, 2008; Leal-Mejia, 2011; Fig. 16). Among these, three metallogenic zones of Miocene to Pleistocene age are recognized: the Middle Cauca belt, the Cauca-Nariño belt, and the California-Vetas district. Besides the La Colosa porphyry gold deposit, the Middle Cauca belt includes porphyry Au-Cu (e.g., Titiribi, Leal-Mejia, 2011; Quinchia, Bissig et al., 2017), porphyry Cu-Au-(Mo) (Nuevo Chaquiro, Bartos et al., 2017), and epithermal vein-type Au-Ag deposits (e.g., Marmato, Tassinari et al., 2008; Mendoza and Ordoñez, 2014; Buriticá, Lesage et al., 2013). The California-Vetas district hosts an isolated cluster of porphyry Cu-Mo, porphyry Au-Cu, and epithermal Au-Ag vein systems (Felder et al., 2005; Horner et al., 2010; Mantilla Figueroa et al., 2013; Bissig et al., 2014; Rodríguez Madrid et al., 2017). The Cauca-Nariño belt includes numerous known gold occurrences associated with As-Ag-Sb-Pb-Zn metal signatures spatially associated with middle to late Miocene porphyry stocks such as Berruecos, Dominical, Cerro Gordo, Berruecos, El Vergel, (Leal-Mejia, 2011), and Piedra Sentada (Gomez-Gutierrez and Molano-Mendoza, 2009).

Mineralization in the Middle Cauca belt as well as in the California-Vetas district shows strong structural control, which is linked to the tectonic reorganization in the North Andean region during the mid-Miocene, when the Panamá-Chocó block docked against the South American continent. As is the case for La Colosa within the Palestina fault system, other known ore deposits in the Middle Cauca belt are associated with regional N- to NNE-striking fault systems, such as the Romeral and Cauca faults (e.g., Nuevo Chaquiro, Marmato, and Buriticá). As mentioned above, in several of these deposits, reversal of the general shear sense from right to left lateral has been proposed or confirmed (e.g., Rossetti and Colombo, 1999; Sillitoe, 2008).

It is thus intriguing that the onset of mid-Miocene magmatic activity coincided with slip reversal along these major regional structures in the northern part of the northern Andes. This correlation may have important implications for further exploration of mineralized systems in the Middle Cauca belt.

Summary and Conclusions

The following conclusions can be drawn from this study:

1. The La Colosa deposit is located within the Tahamí terrane of the Central Cordillera of Colombia. Metamorphosed and deformed Mesozoic rocks of volcano-sedimentary origin (Cajamarca Complex) constitute the country rocks. Two ductile deformation events have been identified within this Complex. The first is characterized by tight, W-vergent folding and development of a penetrative foliation and shallow N- and S-plunging fold axes. The second event, overprinting the first in the western part of the La Colosa area, shows open folding with E- to SE-plunging fold axes and shallow E-dipping shear zones.
2. The regional NNE-striking Palestina fault system crosses the entire deposit area. The fault system is composed of several fault strands and intermediate splays. Like the adjacent Romeral fault system, the Palestina system reversed its slip direction from right lateral to left lateral due to a major change in the stress regime during the docking of the Panamá-Chocó block to South America in the mid-Miocene. The slip reversal reactivated older structures and formed new brittle, extensional structures.
3. Within the regional Palestina fault system, the La Colosa deposit is located in a pull-apart structure that formed upon brittle reactivation of old ductile features and the generation of secondary Riedel shears.
4. This extensional zone favored emplacement of the composite magmatic stocks of the La Colosa intrusive complex. The complex is composed of three main intrusive pulses denoted early, intermineral, and late stage.
5. The porphyry stock was emplaced during a short time span of approximately 1.1 m.y. between ~8.5 and ~7.4 Ma. Re-Os dating at La Colosa suggests that hydrothermal molybdenite mineralization occurred simultaneously with emplacement of the early, intermineral, and late porphyry stocks (8.24 ± 0.08–8.18 ± 0.06 Ma). Consistent with this, K-Ar closure ages of secondary biotite indicate that the La Colosa deposit cooled through 300° to 400°C at 8.0 ± 0.8 and 7.9 ± 0.8 Ma. In contrast, at the San Antonio porphyry stock the Re-Os ages indicate a later mineralization event at 3.24 Ma.
6. Potassic alteration is the dominant alteration type in the La Colosa porphyry stock. The schistose country rock also shows weak to strong potassic alteration accompanied by multiple stages of silicification. Pyrite is the dominant sulfide in the gold-rich (1.5–2.0 g/t Au) zones of the deposit. Pyrrhotite forms an aureole in the country rock. Close to the contact, pyrite and pyrrhotite coexist. Late-stage quartz-sericite alteration is associated with N-trending normal faults.
7. The early porphyry intrusions have the highest gold contents inside the 0.5 g/t Au shell. This gold-rich zone lies above and overlaps a zone of magnetite, chalcopyrite, and molybdenite that is present in the deepest explored portion of the deposit.
8. Following emplacement of the stocks and the porphyry-type Au-Cu-Mo mineralization, continued extensional deformation during uplift of the Central Cordillera formed a set of N-trending normal faults. These faults were sites for renewed hydrothermal fluid flow and deposition of the second, high-grade Au mineralization within sheeted, drusy quartz veinlets bordered by sericite-albite halos. These veinlets crosscut the early, intermineral, and late porphyry intrusions as well the country rocks in the northern area of the La Colosa deposit.
9. Most of the known gold deposits in the Central Cordillera, including La Colosa, belong to the Middle Cauca metallogenic belt. These deposits are all associated with late Miocene (10–6 Ma) intrusive stocks (Leal-Mejia, 2011; Mantilla Figueroa et al., 2013; Bissig et al., 2014; Bartos et al., 2017).

Acknowledgments

Mineral discovery and prefeasibility projects are always the products of successful teamwork. We thank AngloGold Ashanti for giving us the opportunity to present this study, which summarizes the work of numerous geologists involved

in the exploration program and prefeasibility study: Timoleon Garzon, Edwin Palacio, Anwuar Urquiza, William Pulido, German Gonzalez, Cesar Garcia, Javier Gil, Andrés Giraldo, Geronimo Valencia, Daniel Saenz, Andres Rodriguez, Juan Pablo Valencia, Luis Arteaga, Andres Cepeda, Felipe Rodriguez, Mayeli Gomez, Paula Montoya, and Jennifer Betancourt. The initial mineralization model was constructed by Richard H. Sillitoe and Ruben Padilla in 2007. Their training over years produced a generation of porphyry gold geologists. AngloGold Ashanti greatly supported the training in 3-D modeling and geostatistical analysis. The authors are thankful for the discussions and validations with Vaughan Chamberlain and Tim Thompson, in particular, on improving the quality of 3-D models and the exploration benefits during the drilling phases. We gratefully acknowledge Richard Sillitoe, David John, and Stuart Simmons for their critical and constructive comments that helped to improve the manuscript.

REFERENCES

Acosta, J., Lonergan, L., and Coward, M.P., 2004, Oblique transpression in the western thrust front of the Colombian Eastern Cordillera: Journal of South American Earth Sciences, v. 17, p. 181–194.

Alvarado, A., Audin, L., Nocquet, J.M., Jaillard, E., Mothes, P., Jarrín, P., Segovia, M., Rolandone, F., and Cisneros, D., 2016, Partitioning of oblique convergence in the northern Andes subduction zone: Migration history and the present-day boundary of the North Andean Sliver in Ecuador: Tectonics, v. 35, p. 1048–1065.

AngloGold Ashanti, 2016, Mineral resource and ore reserve report 2016, www.aga-reports.com/16/download/AGA-RR16.pdf.

Aspden, J.A., and McCourt, W.J., 1986, Mesozoic oceanic terrane in the central Andes of Colombia: Geology, v. 14, p. 415–418.

Barat, F., Mercier de Lépinay, B., Sosson, M., Müller C., Baumgartner, P.O., and Baumgartner-Mora, C., 2014, Transition from the Farallon plate subduction to the collision between South and Central America: Geological evolution of the Panama Isthmus: Tectonophysics, v. 622, p. 145–167.

Bartos, P.J., García, C., and Gil, J., 2017, The Nuevo Chaquiro Co-Au-(Mo) porphyry deposit, Middle Cauca belt, Colombia: Geology, alteration, mineralization: Economic Geology, v. 112, p. 275–294.

Bayona, G., Cortés, M., Jaramillo, C., Ojeda, G., Aristizabal, J.J., and Reyes-Harker, A., 2008, An integrated analysis of an orogen-sedimentary basin pair: Latest Cretaceous-Cenozoic evolution of the linked Eastern Cordillera orogen and the Llanos foreland basin of Colombia: Geological Society of America Bulletin, v. 120, p. 1171–1197.

Bayona, G., Cardona, A., Jaramillo, C., Mora, A., Montes, C., Valencia, V., Ayala, C., Montenegro, O., and Ibañez-Mejia, M., 2012, Early Paleogene magmatism in the northern Andes: Insights on the effects of oceanic plateau-continent convergence: Earth and Planetary Science Letters, v. 331–332, p. 97–111.

Betancourt, J., 2014, Magmatic evolution of the La Colosa porphyry cluster and related gold mineralization. La Colosa project, Central Cordillera, Colombia: M.S. thesis, Barcelona, University of Barcelona, 34 p.

Bissig, T., Mantilla Figueroa, L.C., and Hart, C.J.R., 2014, Petrochemistry of igneous rocks of the California-Vetas mining district, Santander, Colombia: Implications for northern Andean tectonics and porphyry Cu (-Mo, Au) metallogeny: Lithos, v. 200–201, p. 355–367.

Bissig, T., Leal-Mejía, H., Stevens, R.B., and Hart, C.J.R., 2017, High Sr/Y magma petrogenesis and the link to porphyry mineralization as revealed by garnet-bearing I-type granodiorite porphyries of the Middle Cauca Au-Cu belt, Colombia: Economic Geology, v. 112, p. 551–568.

Blanco-Quintero, I.F., García-Casco, A., Toro, L.M., Moreno, M., Ruiz, E.C., Vinasco, C.J., Cardona, A., Lázaro, C., and Morata, D., 2014, Late Jurassic terrane collision in the northwestern margin of Gondwana (Cajamarca Complex, eastern flank of the Central Cordillera, Colombia): International Geology Review, v. 15, p. 1852–1872.

Borrero, C., Toro, L.M., Alvarán, M., and Castillo, H., 2009, Geochemistry and tectonic controls of the effusive activity related with the ancestral Nevado del Ruiz volcano, Colombia: Geofísica Internacional, v. 48, p. 149–169.

Burke, K, Cooper, C., Dewey, J.F., Mann, P., and Pindell, J.L.,1984, Caribbean tectonics and relative plate motions: Geological Society of America Memoir 162, p. 31–63.

Cediel, F., Shaw, R.P., and Cáceres, C., 2003, Tectonic assembly of the northern Andean block: American Association of Petroleum Geologists (AAPG) Memoir 79, p. 815–848.

Coates, A.G., Collins, L.S., Aubry, M.-P., and Berggren, W.A., 2004, The geology of the Darian, Panama, and the late Miocene-Pliocene collision of the Panama arc with northwestern South America: Geological Society of America Bulletin, v. 116, p. 1327–1344.

Cochrane, R., 2013, U-Pb thermochronology, geochronology, and geochemistry of NNW South America: Rift to drift transition, active margin dynamics, and implications for the volume balance, Ph.D. thesis, Geneva, University of Geneva, 191 p.

Colmenares, L. and Zoback, M.D., 2003, Stress field seismotectonics of northern South America: Geology, v. 31, p. 721–724.

Corredor, F., 2003, Seismic strain rates and distributed continental deformation in the northern Andes and three-dimensional seismotectonics of northwestern South America: Tectonophysics, v. 372, p. 147–166.

Cortés, A., and Angelier, J., 2005, Current state of stress in the northern Andes as indicated by focal mechanisms of earthquakes: Tectonophysics, v. 403, p. 29–58.

Cortés, M., Colletta, B., and Angelier, J., 2006, Structure and tectonics of the central segment of the Eastern Cordillera of Colombia: Journal of South American Earth Sciences, v. 21, p. 437–465.

Egbue, O., and Kellogg, J., 2010, Pleistocene to present North Andean "escape": Tectonophysics, v. 489, p. 248–257.

Ego, F., Sébrier, M., Lavenu, A., Yepes, H., and Egues, A., 1996, Quaternary state of stress in the northern Andes and the restraining bend model for the Ecuadorian Andes: Tectonophysics, v. 259, p. 101–116.

Farris, D.W., Jaramillo, C., Bayona, G., Restrepo-Moreno, S.A., Montes, C., Cardona, A., Mora, A., Speakman, R.J., Glascock, M.D., and Valencia, V., 2011, Fracturing of the Panamanian Isthmus during initial collision with South America: Geology, v. 39, p. 1007–1010.

Felder, F., Ortíz, G., Campos, C., Monsalve, I., and Silva, A., 2005, Angostura project: A high-sulfidation gold-silver deposit located in the Santander Complex of Northeastern Colombia: Pro-Explo, Instituto de Ingenieria del Perú, Lima, May 2005, Proceedings, 15 p.

Gil, J.R., 2010, Igneous petrology of the La Colosa gold-rich porphyry system, Tolima, Colombia: M.S. thesis, Tucson, Arizona, University of Arizona, 51 p.

Gómez, E., Jordan, T.E., Allmendinger, R.W., Hegarty, K., and Kelley, S., 2005a, Syntectonic Cenozoic sedimentation in the northern Middle Magdalena Valley basin of Colombia and implications for exhumation of the northern Andes: Geological Society of America Bulletin, v. 117, p. 547–569.

Gómez, E., Jordan, T.E., Allmendinger, R.W., and Cardozo, N., 2005b, Development of the Colombian foreland-basin system as a consequence of diachronous exhumation of the northern Andes: Geological Society of America Bulletin, v. 117, p. 1272–1292.

Gomez-Gutierrez, D., and Molano-Mendoza, J., 2009, Evaluación de zonas de alteración hidrotermal y fases intrusivas, para el prospecto "Stock porfiritico de Piedra Sentada," Cauca, Colombia: Geología Colombiana, no. 34, p. 75–94.

Gustafon, L., and Hunt, J., 1975, The porphyry copper deposit at El Salvador, Chile: Economic Geology, v. 70, p. 857–912.

Horner, J., Calderón, A., Castro, E., Ortíz, G., Nolasco, T., Castro, W., Silva, A., González, J., and Felder, F., 2010, Angostura gold-silver mining project, Santander, Colombia—geotechnical open-pit design (prefeasibility study): Sociedad Colombiana de Geotécnia, Congreso Nacional, Bogotá, 2010, Proceedings, 7 p.

Horner, J., Naranjo, A., and Weil, J., 2016, Digital data acquisition and 3-D structural modelling for mining and civil engineering—the La Colosa gold mining project, Colombia: Geomechanics and Tunnelling, v. 9, p. 52–57.

Ingeominas, 2006, Mapa Geológico de Colombia, Bogotá, Colombia, scale 1:2,800,000.

Kellogg, J., and Vega, V., 1995, Tectonic development of Panama, Costa Rica, and the Colombian Andes: Constraints from global positioning system geodetic studies and gravity: Geological Society of America Special Paper 295, p. 75–90.

Leal-Mejía, H.M., 2011, Phanerozoic gold metallogeny in the Colombia Andes: A tectono-magmatic approach: Ph.D. thesis, Barcelona, Spain, University of Barcelona, 1000 p.

Leichliter, S., 2013, Gold deportment and geometallurgical recovery model for the La Colosa, porphyry gold deposit, Colombia: M.S. thesis, Hobart, Tasmania, University of Tasmania, 201 p.

Lesage, G., Richards, J.P., Mühlenbachs, K., and Spell, T.L., 2013, Geochronology, geochemistry, and fluid characterization of the late Miocene Buriticá gold deposit, Antioquia Department, Colombia: Economic Geology, v. 108, p. 1067–1097.

Lodder, C., Padilla, R., Shaw, R., Garzon, T., Palacio, E., and Jahoda, R., 2010, Discovery history of the La Colosa gold porphyry deposit, Cajamarca, Colombia: Society of Economic Geologists Special Publication 15, p. 19–28.

Londoño, J.M., 2016, Evidence of recent deep magmatic activity at Cerro Bravo-Cerro Machín volcanic complex, central Colombia: Implications for future volcanic activity at Nevado del Ruiz, Cerro Machín, and other volcanoes: Journal of Volcanology and Geothermal Research, v. 324, p. 156–168.

Ludwig K.R., 2012, User's manual for Isoplot 3.75. A geochronological toolkit for Microsoft Excel: Berkeley Geochronology Center, Special Publication 5, p. 75.

Mantilla Figueroa, L.C., Bissig, T., Valencia, V., and Hart, C.J.R., 2013, The magmatic history of the Vetas-California mining district, Santander massif, Eastern Cordillera, Colombia: Journal of South American Earth Sciences, v. 45, p. 235–249.

Martens, U., Restrepo, J.J., Ordóñez-Carmona, O., and Correa-Martínez, A.M., 2014, The Tahamí and Anacona terranes of the Colombian Andes: Missing links between the South American and Mexican Gondwana margins: Journal of Geology, v. 122, p. 507–530.

Mendoza, F.A., and Ordoñez, O., 2014, Structural controls and evolution of epithermal (Au) and porphyry (Au-Cu)-related systems: Northern Middle Cauca belt district, Colombia: SEG 2014: Building Exploration Capability for the 21st Century, Society of Economic Geologists, Keystone, Colorado, September 27–30, 2014, Proceedings.

Meschede, M., and Frisch, W., 1998, A plate-tectonic model for the Mesozoic and early Cenozoic history of the Caribbean plate: Tectonophysics, v. 296, p. 269–291.

Mora-Bohórquez, J.A., Ibánez-Mejía, M., Oncken, O., de Freitas, M., Vélez, V., Mesa, A., and Serna, L., 2017, Structure and age of the Lower Magdalena Valley basin basement, northern Colombia: New reflection-seismic and U-Pb-Hf insights into the termination of the central Andes against the Caribbean basin: Journal of South American Earth Sciences, v. 74, p. 1–26.

Moreno, C.J., Horton, B.K., Caballero, V., Mora, A., Parra, M., and Sierra, J., 2011, Depositional and provenance record of the Paleogene transition from foreland to hinterland basin evolution during Andean orogenesis, northern Middle Magdalena Valley basin, Colombia: Journal of South American Earth Sciences, v. 32, p. 246–263.

Moreno-Sanchez, M., and Pardo-Trujillo, A., 2003, Stratigraphical and sedimentological constraints on western Colombia: Implications on the evolution of the Caribbean plate: American Association of Petroleum Geologists (AAPG) Memoir 79, p. 891–924.

Moreno-Sanchez, M., Gómez-Cruz, A.de J., and Toro, L.M., 2008, Proveniencia del material del Complejo Quebradagrande y su relación con los complejos adyacentes: Boletín de Ciencias de la Tierra, v. 22, p. 27–38.

Nie, J., Horton, B.K., Mora, A., Saylor, J.E., Housh, T.B., Rubiano, J., and Naranjo, J., 2010, Tracking exhumation of Andean ranges bounding the Middle Magdalena Valley basin, Colombia: Geology, v. 38, p. 451–454.

Nivia, A., Marriner, G., Kerr, A., and Tarney, J., 2006, The Quebradagrande Complex: A Lower Cretaceous ensialic marginal basin in the Central Cordillera of the Colombian Andes: Journal of South American Earth Science, v. 21, p. 423–436.

Ordoñez-Carmona, O., Restrepo Álvarez, J.J., Martins Pimentel, M., 2006, Geochronological and isotopical review of pre-Devonian crustal basement of the Colombian Andes: Journal of South American Earth Sciences, v. 21, p. 372–382.

Parra, M., Mora, A., Lopez, C., Rojas, L.E., and Korton, B., 2012, Detecting earliest shortening and deformation advance in thrust belt hinterlands: Example from the Colombian Andes: Geology, v. 40, p. 175–178.

Restrepo, J.J., Ordoñez-Carmona, O., Armstrong, R., and Pimentel, M.M., 2011, Triassic metamorphism in the northern part of the Tahamí terrane of the Central Cordillera of Colombia: Journal of South American Earth Sciences, v. 32, p. 497–507.

Rodriguez, C., and Warden, A.J., 1993, Overview of some Colombian gold deposits and their development potential: Mineralium Deposita, v. 28, p. 47–57.

Rodríguez Madrid, A.-L., Bissig, T., Hart, C.J.R., and Mantilla-Figueroa, L.C., 2017, Late Pliocene high-sulfidation epithermal gold mineralization at the La Bodega and La Mascota deposits, Northeastern Cordillera of Colombia: Economic Geology, v. 112, p. 347–374.

Rossetti, P., and Colombo, F., 1999, Adularia-sericite gold deposits of Marmato (Caldas, Colombia): Field and petrographical data: Geological Society, London, Special Publications, v. 155, p. 167–182.

Sarmiento-Rojas, L.F., Van Wess, J.D., and Cloetingh, S., 2006, Mesozoic transtensional basin history of the Eastern Cordillera, Colombian Andes: Inferences from tectonic models: Journal of South American Earth Sciences, v. 21, p. 383–411.

Saylor, J.E., Horton, B.K., Nie, J., Corredor, J., and Mora, A., 2010, Evaluating foreland basin partitioning in the northern Andes using Cenozoic fill of the Floresta basin, Eastern Cordillera, Colombia: Basin Research, v. 23, p. 377–402.

Seedorff, E., Dilles, J., Proffett, J., and Einaudi, M., 2005, Porphyry deposits: Characteristics and origin of hypogene features: Economic Geology 100th Anniversary Volume, p. 251–298.

Sillitoe, R.H., 1985, Ore-related breccias in volcanoplutonics arc: Economic Geology, v. 80, p. 1467–1514.

——2000, Gold-rich porphyry deposits: Descriptive and genetic models and their role in exploration and discovery: Reviews in Economic Geology, v. 13, p. 315–345.

——2008, Major gold deposits and belts of the North and South American Cordillera: Distribution, tectonomagmatic setting, and metallogenic considerations: Economic Geology, v. 103, p. 663–687.

Sillitoe, R.H., Jaramillo, L., Damon, P.E., Shafiqullah, M., and Escovar, R., 1982, Setting, characteristics, and age of the Andean porphyry copper belt in Colombia: Economic Geology, v. 77, p. 1837–1850.

Spikings, R., and Simpson, G., 2014, Rock uplift and exhumation of continental margins by collision, accretion, and subduction of buoyant and topographically prominent oceanic crust: Tectonics, v. 33, p. 633–655.

Spikings, R., Cochrane, R., Villagomez, D, van der Lelij, R., Vallejo, C., Winkler, W., and Beate, B., 2015, The geological history of northwestern South America: From Pangea to early collision of the Caribbean large igneous province (290–75 Ma): Gondwana Research, v. 27, p. 95–139.

Taboada, A., Rivera, L.A., Fuenzalida. A., Cisternas, A., Philip, H., Bijwaard, H., Olaya, J., and Rivera, C., 2000, Geodynamics of the northern Andes: Subductions and intracontinental deformation: Tectonics, v. 19, p. 787–813.

Tassinari, C., Diaz, F., and Buenaventura, J., 2008, Age and sources of gold mineralization in the Marmato mining district, NW Colombia: A Miocene-Pliocene epizonal gold deposit: Ore Geology Reviews, v. 33, p 505–518.

Van der Lelij, R., Spikings, R., and Mora, A., 2016, Thermochronology and tectonics of the Mérida Andes and the Santander massif, NW South America: Lithos, v. 248–251, p. 220–239.

Vargas, C.A., and Mann, P., 2013, Tearing and breaking off subducted slabs as the result of collision of the Panama arc-indenter with northwestern South America: Bulletin of the Seismological Society of America, v. 103, p. 2025–2046.

Vargas, C.A., Kammer, A., Valdes, M., Rodriguez, C., Caneva, A., Sanchez, J.J., Arias, E., Cortes, C., and Mora, H., 2005, New geological and geophysical contributions in the section Ibague-Armenia, Central Cordillera, Colombia: Earth Sciences Research Journal, v. 9, no. 2, p. 99–109.

Veloza, G., Styron, R., and Taylor, M., 2012, Open-source archive of active faults for northwest South America: GSA Today, v. 22, p. 4–10.

Villagómez, D., and Spikings, R., 2013, Thermochronology and tectonics of the Central and Western Cordilleras of Colombia: Early Cretaceous-Tertiary evolution of the northern Andes: Lithos, v. 160–161, p. 228–249.

Villagómez, D., Spikings, R., Magna, T., Kammer, A., Winkler, W., and Beltrán, A., 2011, Geochronology, geochemistry, and tectonic evolution of the Western and Central Cordilleras of Colombia: Lithos, v. 125, p. 875–896.

Andrés Naranjo is chief of exploration at Continental Gold, based out of Medellin, Colombia. He received a bachelor's degree in geology and is currently studying for a master's degree in earth science from Universidad de Caldas, Colombia. Andrés was an exploration geologist with AngloGold Ashanti from 2008 to 2017 and worked 11 years in greenfield exploration, target generation, and drilling advanced projects. He is a member of the Society of Economic Geologists, the Society for Geology Applied to Mineral Deposits, and the Australasian Institute of Mining and Metallurgy.